REPORT TO THE UNITED STATES OFFICE

OF AEROSPACE RESEARCH

DR. J. W. LINNETT,
INORGANIC CHEMISTRY LABORATORY,
OXFORD.

1965.

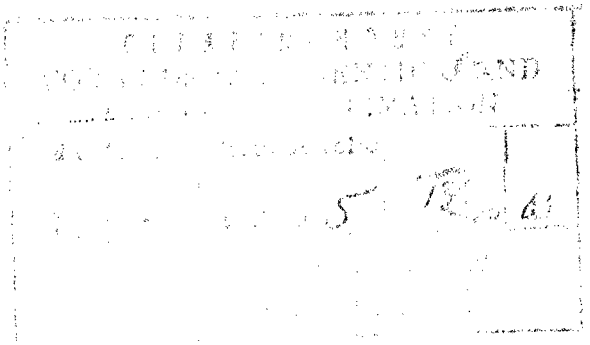

Grant AF EOAR 63-32

FINAL REPORT

March 1965.

"The Reaction of Atoms and Radicals with Various Molecules"

The research supported in this document has been sponsored in whole by:

AIR FORCE OFFICE OF SCIENTIFIC RESEARCH, OAR

through the European Office of Aerospace Research, United States Air Force.

J. W. LINNETT
Inorganic Chemistry Laboratory
University of Oxford,
Oxford, England.

INTRODUCTION.

This report is divided into four chapters:-

Chapter I. deals with some experiments on the Absorption of hydrogen atoms by palladium, and palladium-gold alloys. This work was carried out in connection with some earlier work on the catalytic effect of these metals and alloys on the recombination of hydrogen atoms.

ChapterII. deals with some experiments on the attack of a number of metals by molecular and atomic oxygen to discover in which cases there were considerable differences in rate.

Chapter III. deals with some experiments on the recombination of oxygen atoms on the surface of the alkali metal tungsten bronzes.

Chapter IV. describes a pressure gauge which has been devised for the rapid and convenient measurement of pressures in mixtures containing chlorine at pressures of the order of 1 mm. the accuracy being about $\pm$ 0.01 mm. The experiments on the recombination of chlorine atoms have not yet reached a stage at which a report is worth-while.

In addition, during the period of this grant, work was carried out on the reactions of atoms at metal surfaces. In these experiments oxygen atoms effused through a small hole opposite which was a small disc coated with silver, copper, chromium etc. A complete report of this work was given in the report submitted in December 1963 (pages 1 - 14 of that report). Consequently no further description of that work is included here.

CHAPTER 1.

Absorption of Hydrogen Atoms by Palladium and Palladium Gold Alloys. Introduction. by D. M. Hirst and J. W. Linnett.

Some time ago we made some measurements on the recombination of hydrogen atoms at the surface of palladium, gold and palladium-gold alloys. This work is about to be published in a paper entitled "The Recombination of Atoms on Pd-Au Alloys" by P. G. Dickens, J. W. Linnett and W. Palczewska in the Journal of Catalysis (The work was supported by the Office of Aerospace Research of the U.S. Air Force: Grant: AF EOAR 62-6). It was found that palladium was more active than gold in catalysing the recombination, that small percentages of gold in the palladium did not reduce the initial activity but that larger amounts did. However, another interesting result was that the activity of palladium, and the palladium rich alloys, decreased with time as the foil was exposed to atomic hydrogen. It was concluded that the presence of vacancies in the metallic d-band enhanced the catalytic activity of the materials, but that these vacancies could be filled either by alloying gold with the palladium, or when atomic hydrogen was absorbed by the metal or alloy. That is, when atomic hydrogen was absorbed, its electron was contributed to the completion of the d-band with a consequent fall off in the activity. This hypothesis demands that palladium and its alloys should absorb hydrogen when exposed to hydrogen containing atomic hydrogen under the conditions in which the catalytic experiments were carried out (i.e. hydrogen pressure about 10^{-2} mm.; percentage of atoms about 10%; room temperature). This was the reason why these experiments were carried out. Samples of the metals and alloys

were suspended from a micro-balance and then exposed to hydrogen containing atoms. The increase in weight with time (if any) was followed.

Brief Survey of Related Work.

Palladium is known to absorb large quantitiies of hydrogen. If it is exposed to hydrogen at about 2 atmospheres pressure it will take up about 0.6 gm. atoms of hydrogen for every gram atom of palladium. The hydrogen diffuses as atoms into the palladium lattice. The initial solution produces what is known as the α-phase. This is accompanied by a gradual expansion of the face-centred cubic palladium lattice spacing from about 3.883 to 3.894 A at a concentration of about 0.2 gm. atoms of H per gm. atom of palladium. At this concentration the lattice suddenly expands to 4.018 A with the formation of the β-phase which is also face centred cubic. The lattice spacing remains constant for concentrations between 0.2 and 0.7 or 0.8 gm. atoms of hydrogen per gm. atom of palladium but at higher concentrations it increases again. Concentrations higher than 0.9 gm. atoms of H per gm atom of palladium do not seem to have been attained. The β-phase can be supersaturated with hydrogen by electrolytic charging, the excess hydrogen being lost when the charging process ceases.

The magnetic susceptibility of palladium decreases linearly with the hydrogen concentration becoming zero when there are about 0.66 gm. atoms of H per gm. atom of palladium. Palladium atoms have 10 electrons beyond the closed core consisting of the 1s, 2s, 2p, 3s, 3p, 3d, 4s and 4p orbitals. The 4d and 5s atomic orbitals produce, in the metal, a broad s-band and a narrow d-band which can accomodate 2 and 10 electrons

respectively. The electrons occupy levels in the two bands up to the same energy level. There are, per atom, 9.4 electrons in the d-band and 0.6 in the s-band. Thus there are about 0.6 holes in the narrow d-band. The electrons of the absorbed hydrogen atoms are presumed to enter these holes in the d-band. Norberg (Phys. Rev., 1952, 86, 745) showed, using nuclear magnetic resonance spectroscopy, that the hydrogen is present in the lattice in the form of protons. The magnetic susceptibility drops to zero when the holes in the d-band are filled.

The kinetics of the absorption of hydrogen by palladium from ordinary hydrogen gas has been investigated by Holt (Proc. Roy. Soc., 1914, 90A, 226), Tammann and Schneider (Z. anorg. Chem. 1928, 172, 43), Smith and Derge (J.A.C.S., 1934, 56, 2313) and Krause and Kahlenberg (Trans. Electrochem. Soc., 1935, 68, 449). Most of the experiments showed that there was a linear rate of uptake initially which was followed by a falling off in the rate as the amount absorbed approached a limiting value. The rate, and the amount taken up were very dependent on the previous treatment.

Palladium and gold produce a continuous series of solid solutions. The structure is face-centred cubic and there is no evidence of a super-lattice. The spacing varies almost exactly in a linear manner with concentration. Vogt (Ann Physik, 1932, 14, 1) found that the magnetic susceptibility decreases as the proportion of gold increases becoming zero at about 55 atomic per cent of gold.

Couper and Eley (Disc. Farady Soc., 1950, 8, 172) studied the ortho-para hydrogen conversion on palladium-gold alloys and obtained results similar in form to those of Dickens, Linnett and Palczewska

for the recombination of hydrogen atoms. Couper and Eley also observed that hydrogen exerted a poisoning effect on the reaction they studied.

Schneiderman (Ann. Physik., 1932, 13, 761) investigated the solubility of hydrogen in palladium-gold alloys. The alloys were charged electrolytically. He showed that the solubility decreased as the gold content increased.

Experimental Method.

The sample of metal or alloy weighing about ½ gm. was suspended in a vertical tube of about 4 cm. in diameter from one arm of a micro-balance capable of measuring a change in weight of 10^{-6} gms. The vertical tube was joined at its lower end to a horizontal tube along which hydrogen at $^1/_{10}$ mm pressure was flowing. This hydrogen had been passed through an electric discharge and so contained atoms. These diffused up the vertical tube to the sample. By this means therefore a steady condition could be maintained indefinitely. That is the flow rate, pressure and proportion of atoms at the lower end of the tube containing the sample was constant for as long as was needed for the experiment. Moreover the apparatus could be left operating unattended.

In order that there should be no contamination by electrode materials, an electrodeless discharge was used. This was maintained by 13½ Mc/s radiation from an R.C.A. radio frequency oscillator (type ET-4336-B), a helix of seven 2" copper tubing being wrapped round the tube through which the hydrogen was flowing. In the discharge region there will be present ions, electrons, atoms and molecules some of which will be in

excited states. The charged species will decay rapidly and will not reach the test region. Because the first excited state of hydrogen atom is more than 10 eV above the ground state and the first excited state of the hydrogen molecules is purely repulsive, it is extremely likely that the gas in the test region will consist of a mixture of atoms and molecules in their ground states.

The hydrogen was prepared by the electrolysis of a 15% solution of sodium hydroxide saturated with barium hydroxide to prevent the evolution of any carbon dioxide. A current of 5 amps from the 100 volt D.C. supply was used and the cell was water-cooled. Any oxygen was removed from the hydrogen by passing through a tube containing palladised asbestos at 400°C. The gas could be dried by passing through a trap cooled in liquid oxygen and then through a column of phosphorus pentoxide. If the gas was needed moist it was passed through a humidifier containing water at a controlled temperature. The flow of the hydrogen was measured by determining the pressure drop across a tube containing a plug of sintered glass wool. The flow of gas from the high pressure (atmospheric) region into the low pressure part was controlled by an Edwards fine control needle valve LBIA. The flow meter, saturator and needle valve were immersed in a water bath maintained at 23°C by a Tecam Tempunit.

The pumping system consisted of a large high speed single stage mercury pump backed by a smaller two stage mercury pump. These were backed by an Edwards "Speedivac" 1S 150 rotary oil pump. The pumping line was made of 4 cm. diameter tubing and contained two large volumes to act as flow stabilisers. A block diagram of the apparatus is shown

in Figure I.1.

The balance used was a Sartorius vacuum Electrono-microbalance. It could operate on seven ranges of sensitivity of 1, 2, 5, 10, 20, 50 and 100 ug per scale division. The results could also be recorded on a Leeds and Northrup "Speedomax H S" recorder. The micro-balance was mounted on a bracket of $\frac{1}{4}$" steel measuring 18" by 6" which was fixed into the wall, 6" being in the wall. A piece of slate, supported on two strips of lead was placed on the bracket. A sheet of fairly hard rubber $\frac{1}{8}$" thick was stuck onto the slate and the micro-balance placed on top of this. The sample was supported by a silica hook which was attached to a silica suspension fibre which was in turn hung from the steel suspension wire on one arm of the balance. A counterweight of approximately the same weight as the sample was hung from the other arm.

The sample was situated in a vertical tube which was 4 cm. in diameter. This tube was of silica and the vertical section was 45 cm. long. It was connected to the microbalance through a flange. This vertical tube was made into a furnace so that the sample could be heated up to 800°C. The temperature was measured with a platinum/platinum-rhodium thermocouple. Additional thermocouples were contained in the tube to measure the temperature gradient in the region of the sample.

The gas pressure was measured with a McLeod gauge with a compression ratio of 1000:1. The atom concentration in the neighbourhood of the sample could be measured with a Wrede-Harteck gauge fused into the wall of the silica tube. The pressures inside and outside the gauge were

measured with micro-Pirani pressure gauges which we constructed.

Experimental Results.

Samples of foil, 2/1000" thick, containing 0, 12, 31, 45, 72 and 100 atomic per cent of gold were used. The alloys were kindly loaned by the Mond Nickel Company.

After a number of rather unsatisfactory experiments with dry gas it was decided to use wet gas. This increases very greatly the production of hydrogen atoms. If any oxygen atoms are formed they will be converted rapidly to OH and H by the reaction

$$O + H_2 = H + OH$$

and any hydroxyl radicals to hydrogen atoms by

$$OH + H_2 \quad H_2O + H.$$

Consequently at the test sample, the material will be exposed to hydrogen molecules and atoms together with a small proportion of water molecules. Experiments were carried out on pure gold with dry gas but on all the other samples with wet gas. The samples weighed about $\frac{1}{2}$ gm. and measured $2\frac{1}{2}$ or 3 cms. by $2\frac{1}{2}$ or 3 cms.

Figure I.2 shows the results for palladium, the increase in weight being plotted against time. In this case the measurements of atom concentration were unreliable but in the 2nd and 5th runs the calculated percentages were $6\frac{1}{2}$ and 5% respectively. Table 1 gives the details of the experiment together with the limiting up-take of hydrogen measured in parts per million (by weight). The results for the palladium-gold alloys are shown in Figures I. 3, 4, 5, 6 and 7 and similar details are included in Table I . The results for gold are shown in Figure I 7 .

Table II lists the limiting amounts of hydrogen taken up by the

different metals and alloys expressed as gm. atoms of hydrogen (x) per mole of alloy, $Pd_yAu_{(1-y)}$. These are plotted against the atomic percentages of gold (i.e. 100(1 - y)%) in the alloy in Figure 1.8.

When the discharge was switched off at the end of a hydrogen-absorption experiment, there was usually a steady decrease in weight. The hydrogen starts to desorb as soon as the source of atoms is removed. Figure 1.9 shows the loss in weight against time for three experiments with palladium. With the alloys the desorption took place in a similar way but the rates of desorption were rather variable from experiment to experiment (initial rates of loss were 40 to 150 gms. per hour).

Under these conditions only a part of the hydrogen was lost. However, if the sample was heated, the rest of the hydrogen could be driven off. When the palladium sample was heated up, the loss started at about 90° or 100°C and took about a quarter or half an hour. With the samples containing 88% and 69% of palladium the results were essentially similar, but with the sample containing 55% palladium, though the loss commenced at 90° it took place rather more slowly.

Discussion.

The most striking feature of these experiments is the enormous absorption of hydrogen which occurs when palladium and palladium-gold alloys containing more than 40 atomic per cent of palladium are exposed to partially dissociated hydrogen at pressures of the order of 0.1 mm. Hg. The absorption from molecular hydrogen is negligable at such pressures.

Because the results are variable it is not possible to reach any very definite conclusions regarding the rate of uptake of hydrogen by the different samples. However there are two rather general comments that can

be made. W. Jost (Diffusion in solids, liquids and gases, Academic Press Inc., New York, 1952) has shown that if the uptake is diffusion controlled then it is to be expected that the function $\log_{10} \frac{\bar{c} - c_f}{c_i - c_f}$ should vary linearly with the time, where c_i and c_f are the initial and final concentrations of absorbed material and $\bar{c}$ is the average concentration at time t. It was found that this is true for the initial up-take of the hydrogen. This is shown for two experiments with the palladium-gold alloy containing 88% palladium in Figure 1.10. Here it is seen that the points lie on a straight line for about the first five hours. Similar results were obtained for other alloys. However, for the later stages, this relation did not hold. It was found that the results were then treated best in terms of diffusion through a film of increasing thickness (analogous to the treatment of the formation of oxides when a coherent film is formed). Under these conditions the square of the weight increase is a linear function of the time. That this holds, at any rate approximately, for two experiments with the same alloy is shown in Figure I.11.

If this is a correct interpretation of the data, then one reaches the conclusion that the up-take of atomic hydrogen must be regarded in the following way. To begin with the hydrogen is taken up and diffused into the metal or alloy, the part containing the hydrogen being a uniform phase together with the metal. Thus the up-take is controlled by a simple diffusion process. However, as more is taken up, the outside layer which now contains a lot of hydrogen becomes a new phase and the build up of this phase from the inner part of the sample is controlled by diffusion of hydrogen atoms through this layer which becomes thicker and thicker with time, the thickness being proportional approximately to the weight

increase. This may be related to the phase changes in the solid, though if these were to be identified simply as the α and β phases one would have expected the change-over from simple diffusional behaviour to occur at a lower hydrogen content.

It was shown that when an alloy was saturated with hydrogen atoms and the source of hydrogen atoms then switched off some hydrogen was lost. It is shown in Figure 1.12 that if $\log \frac{c - c_f}{c_i - c_f}$ is plotted against time for some results for an alloy containing 69% palladium a straight line is obtained. This shows that the process is a diffusional one. It is difficult to see how this is to be linked with the results for the up-take of atomic hydrogen though one must bear in mind that, in the desorption experiment, molecular hydrogen is being lost from the surface.

The results in Figure 8 show that the total amount of hydrogen absorbed decreases as gold is added. It can be concluded that when hydrogen is absorbed the electrons enter the d-band. Also when gold is added the additional electron, beyond the closed shells, enters the d-band - consequently as gold is added the number of vacancies in the d-band decreases and consequently the ability to absorb hydrogen atoms decreases.

It appears from Figure 8 that when 58 atomic per cent of gold has been added the d-band is full and no more hydrogen can be absorbed. This agrees fairly well with the results quoted in the Introduction, namely that, in palladium there are 0.6 holes per atom in the d-band.

These results fall into line with those obtained by Dickens, Linnett and Palczewska on the poisoning effect of both gold and atomic hydrogen on the activity of palladium as a catalyst for the recombination of hydrogen atoms. It seems that high activity is to be associated with

vacancies in the d-band as has been proposed. However the alloy containing 72 atomic per cent of gold does show an activity markedly greater than that of gold which would not be expected on the simple arguments given above. It may be that the electronic conditions at the surface are rather difficult from those in the bulk and that there are d-shell vacancies for the surface atoms when there are essentially no d-band vacancies. Nevertheless, broadly speaking, the present results confirm the interpretation of the earlier catalytic results.

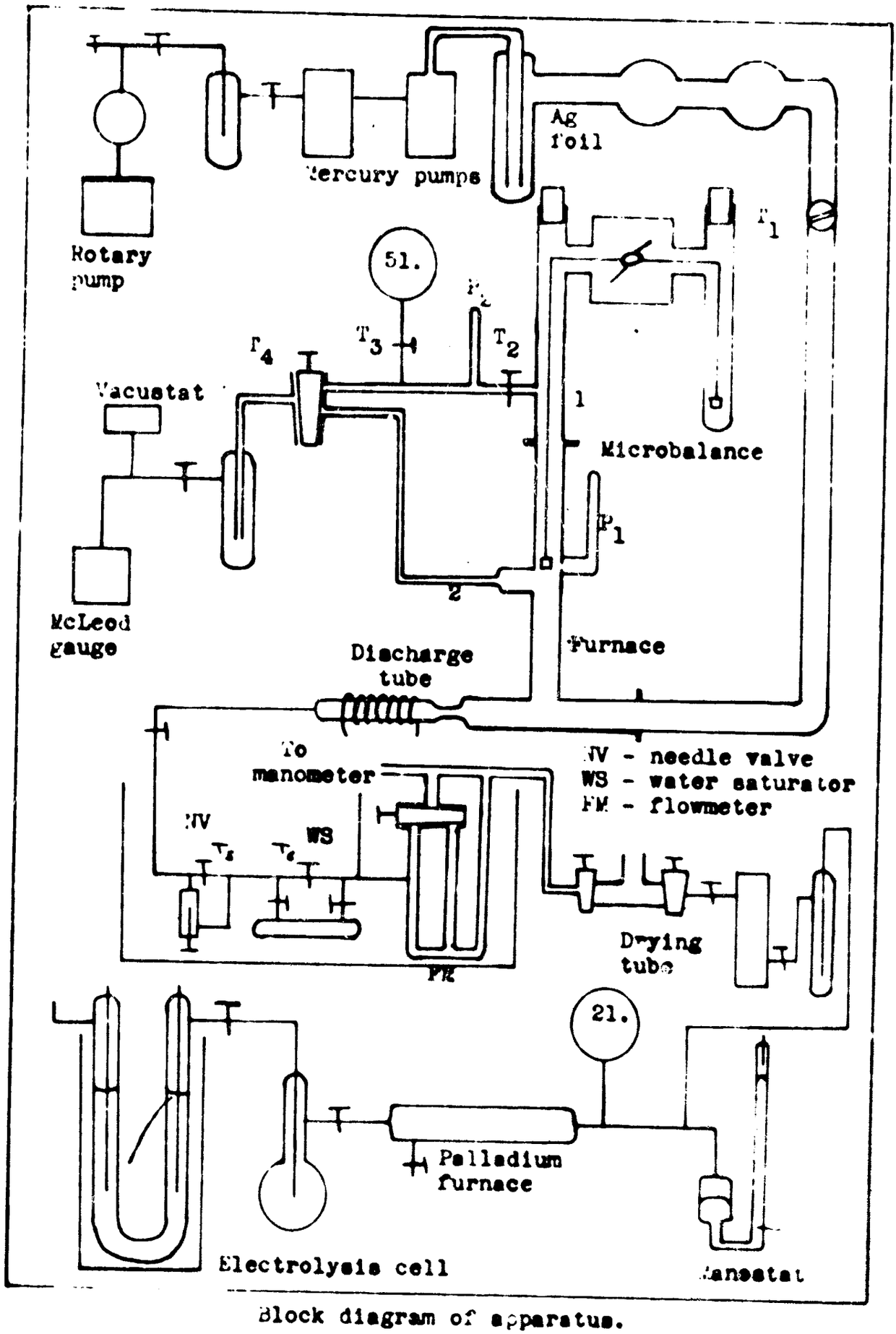

Block diagram of apparatus.

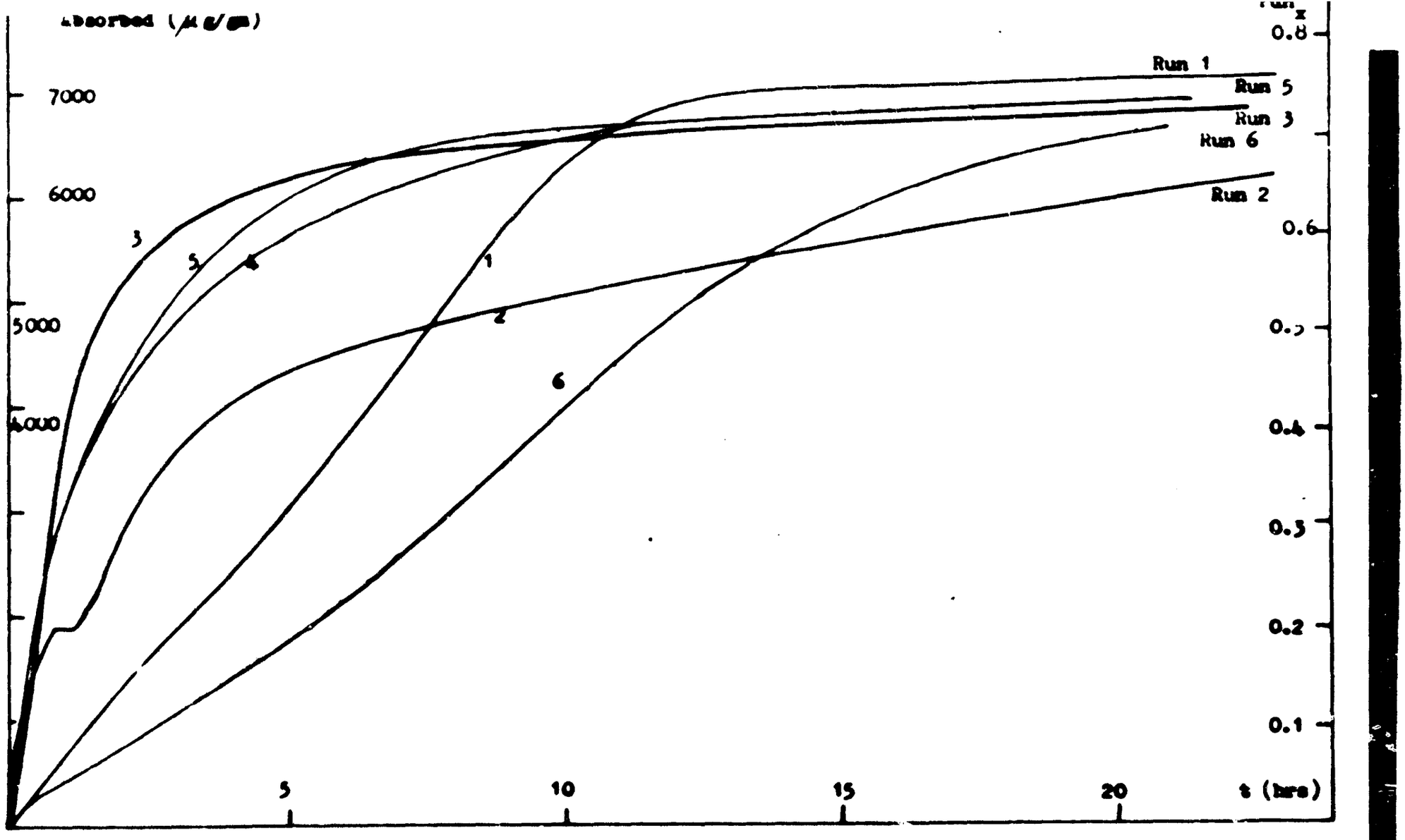

Absorption curves for palladium.

I. 1

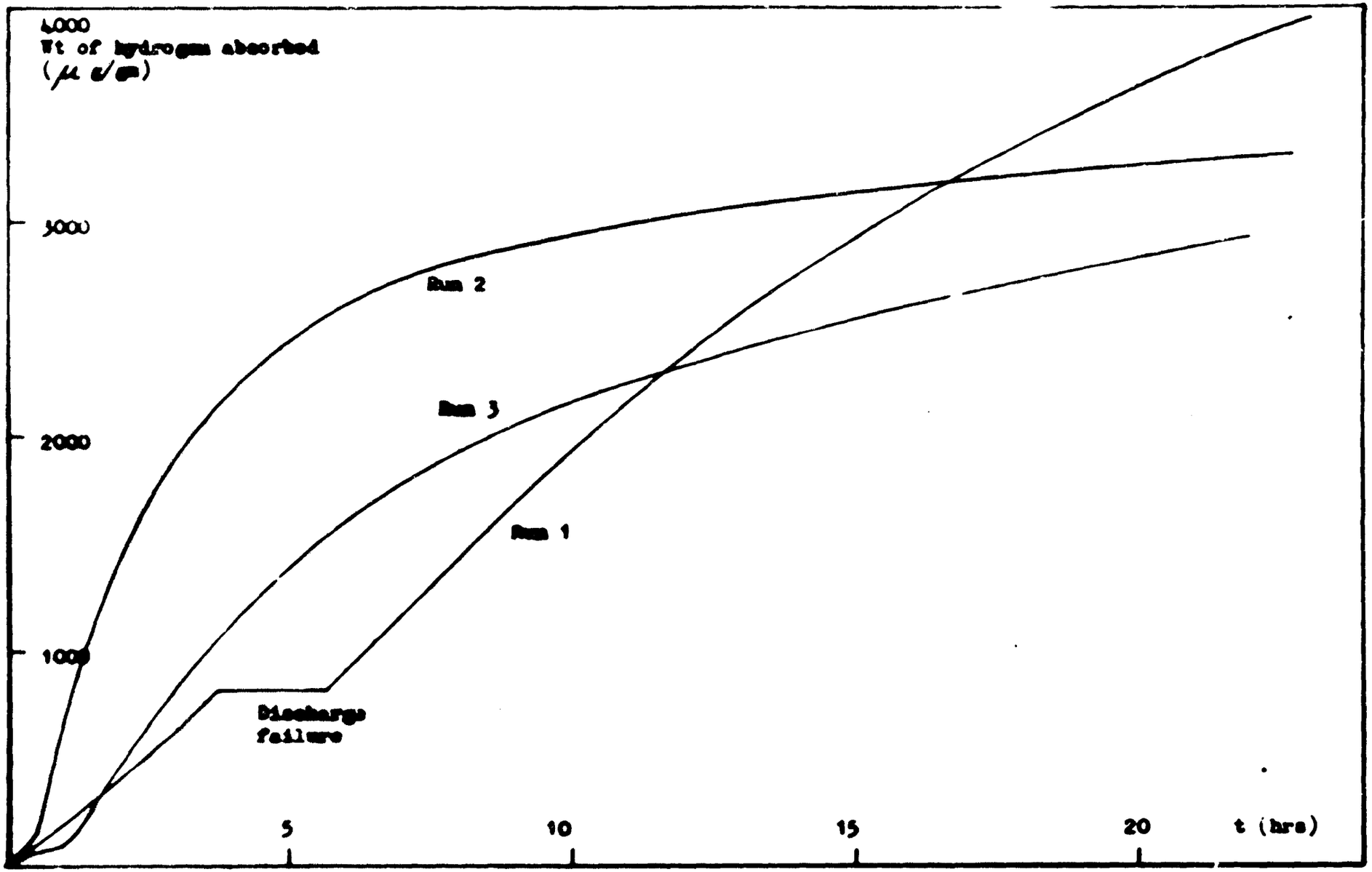

Absorption curves for PdSbAu12.

I.3

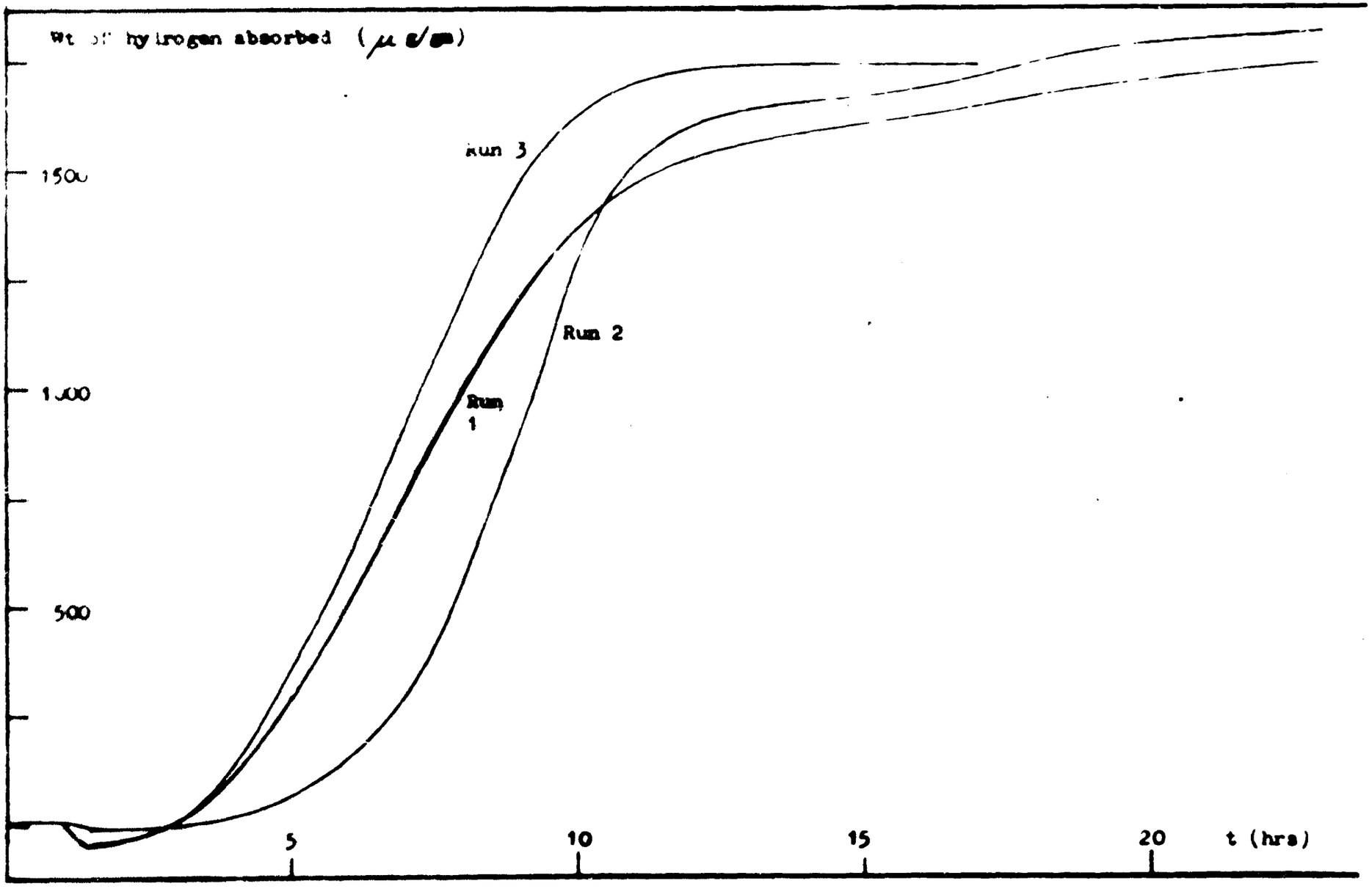

Absorption curves for Pd69Au31.

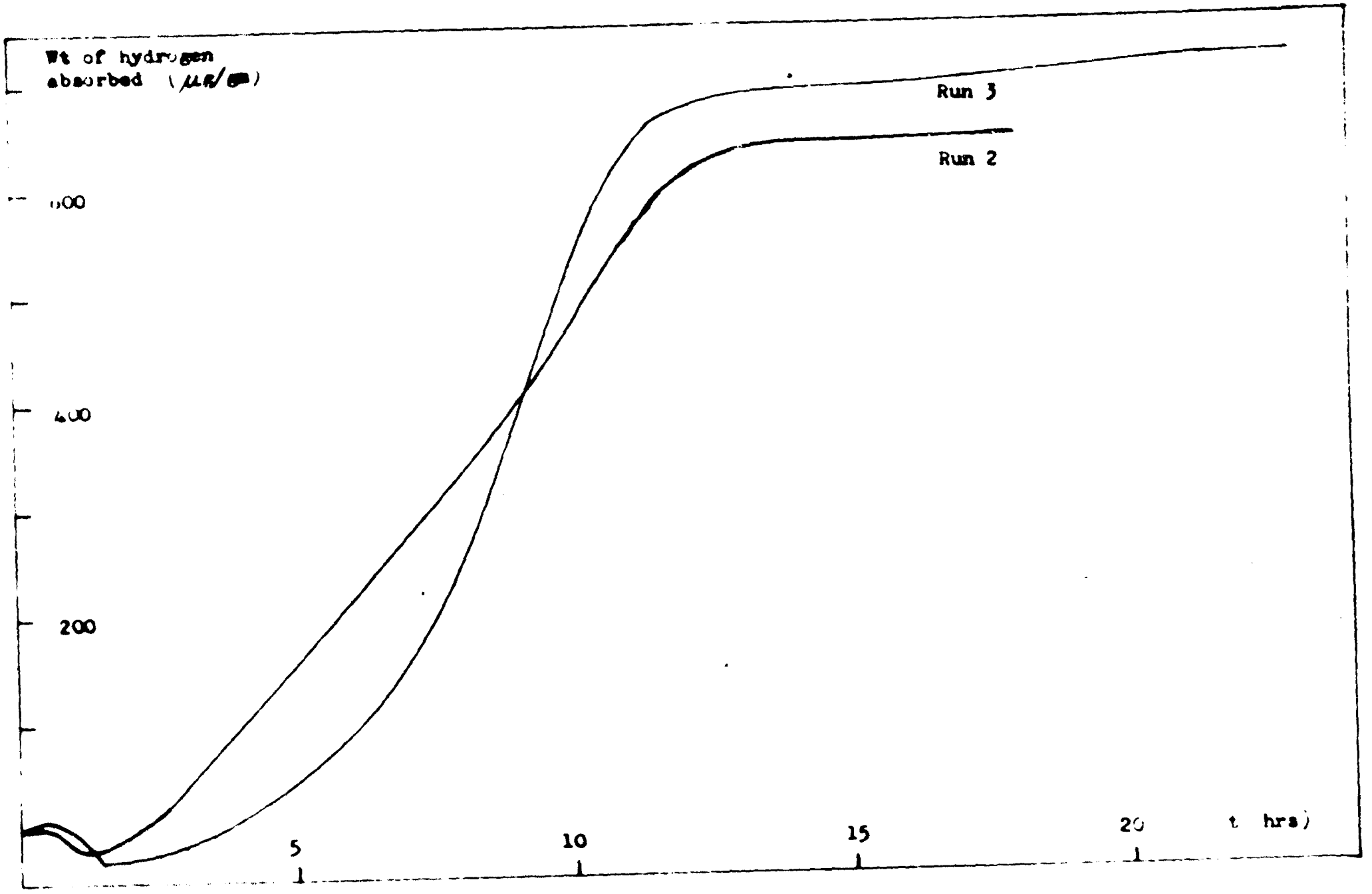

Absorption curves for Pd55Au45.

Variation of weight with time for Pd28Au72 (run2)

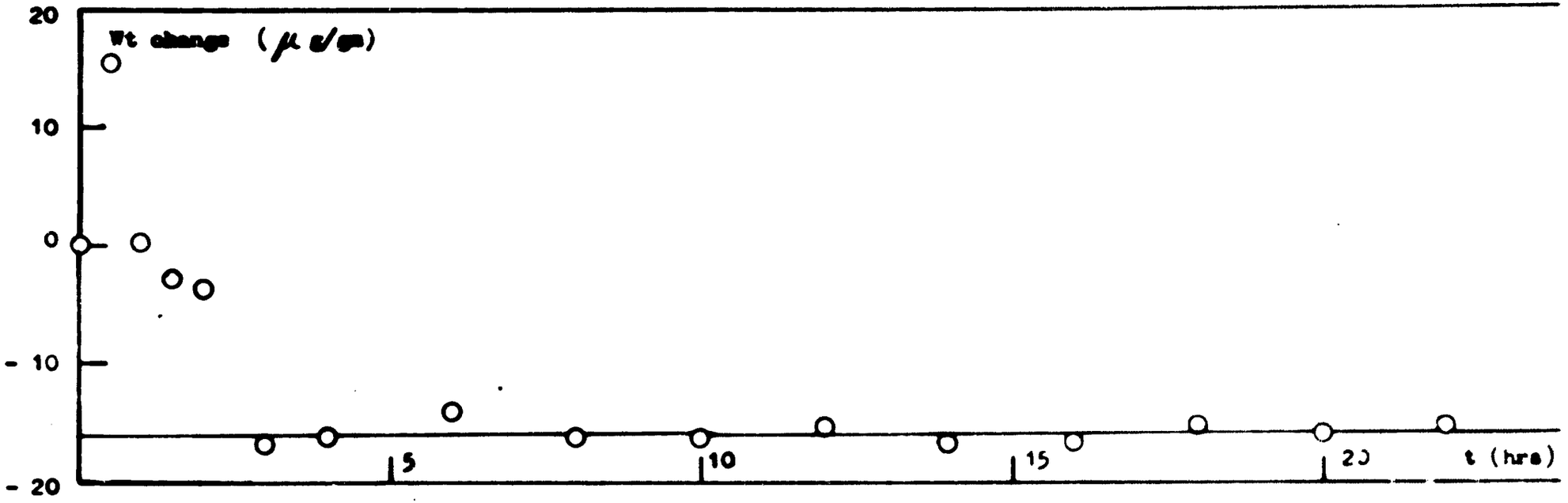

Variation of weight with time for gold (run 2).

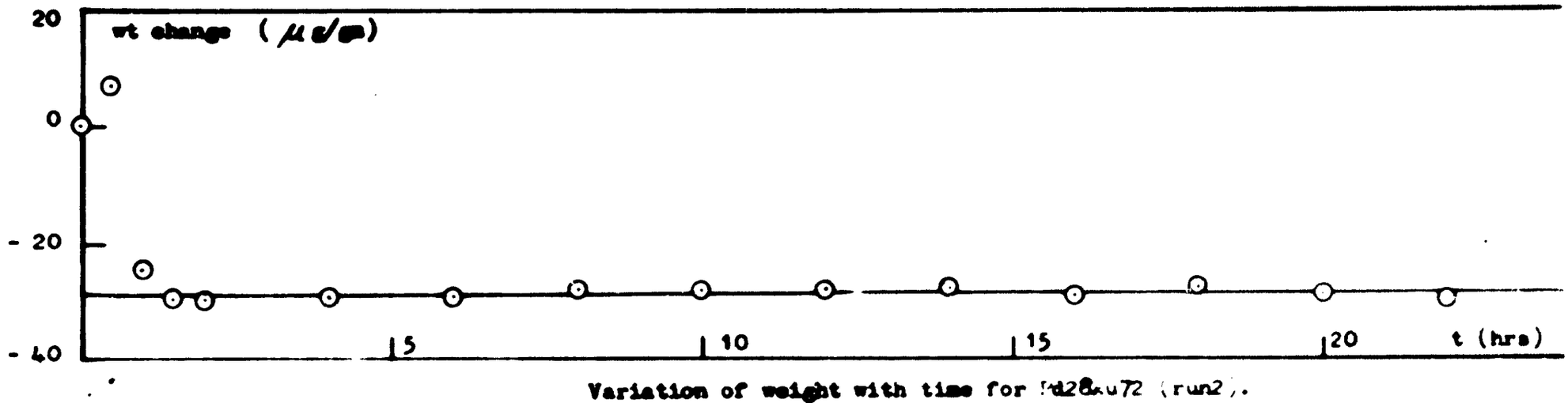

Variation of weight with time for Pd2Au72 (run2).

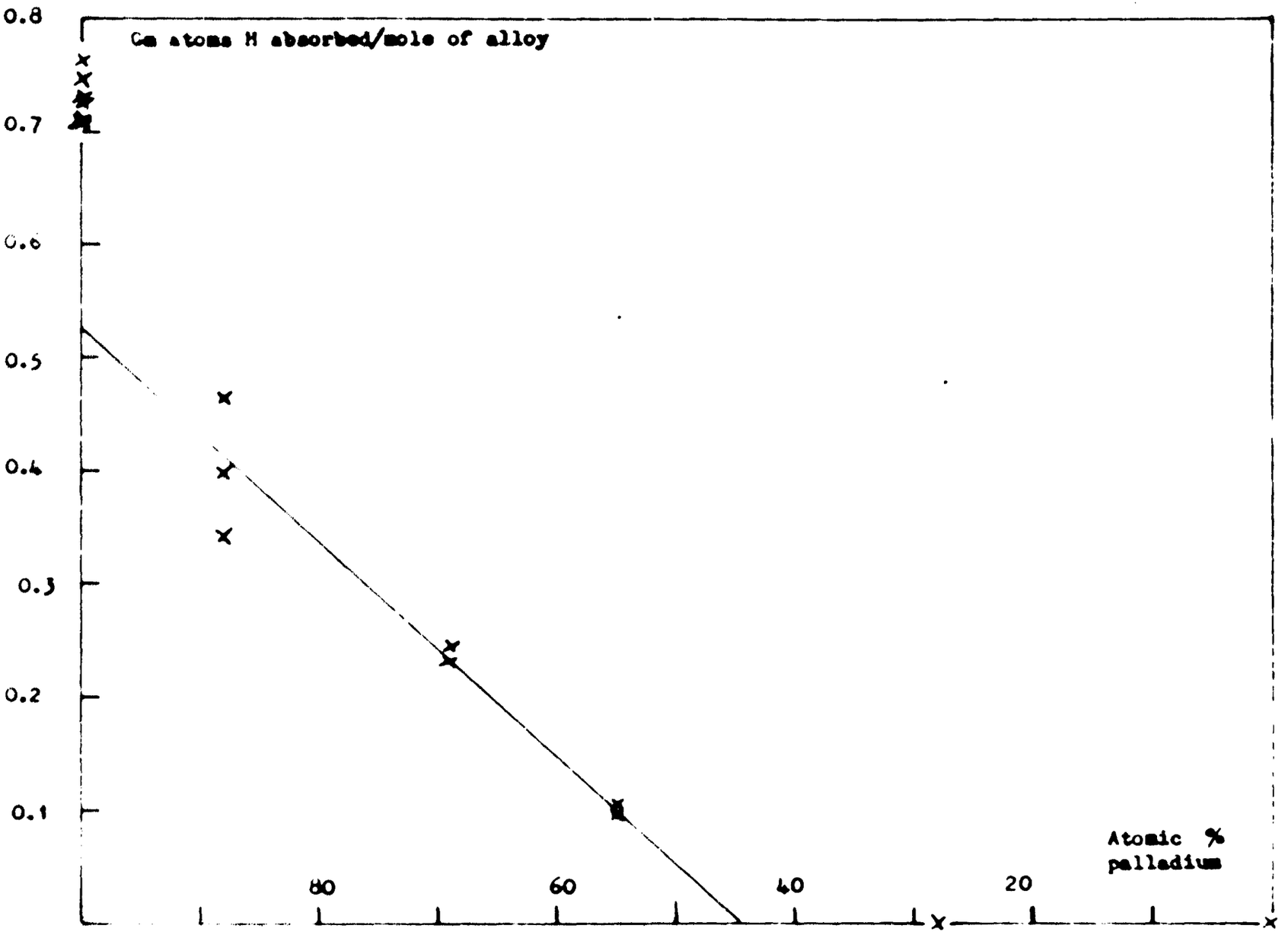

Variation of absorption with alloy composition.

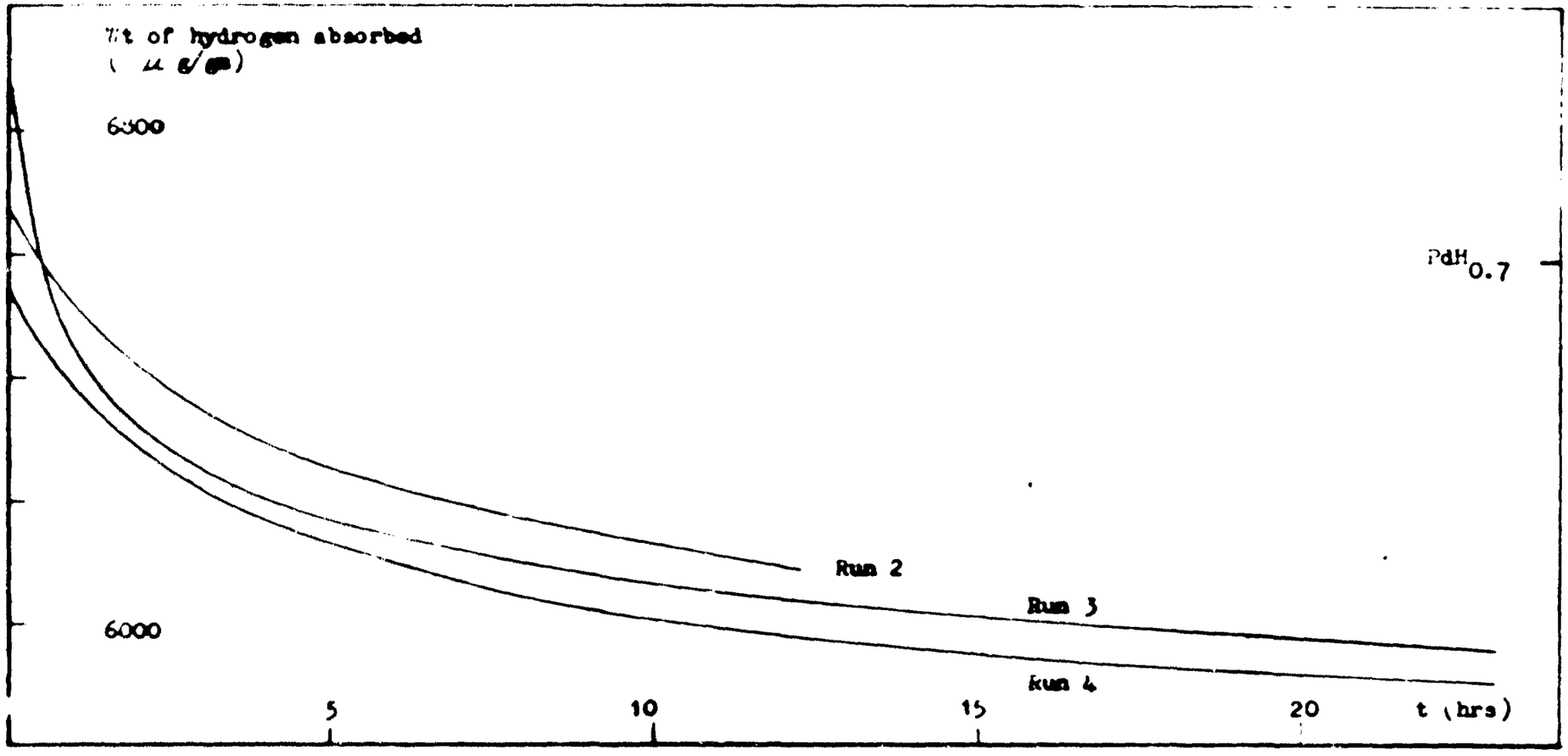

Desorption curves for palladium.

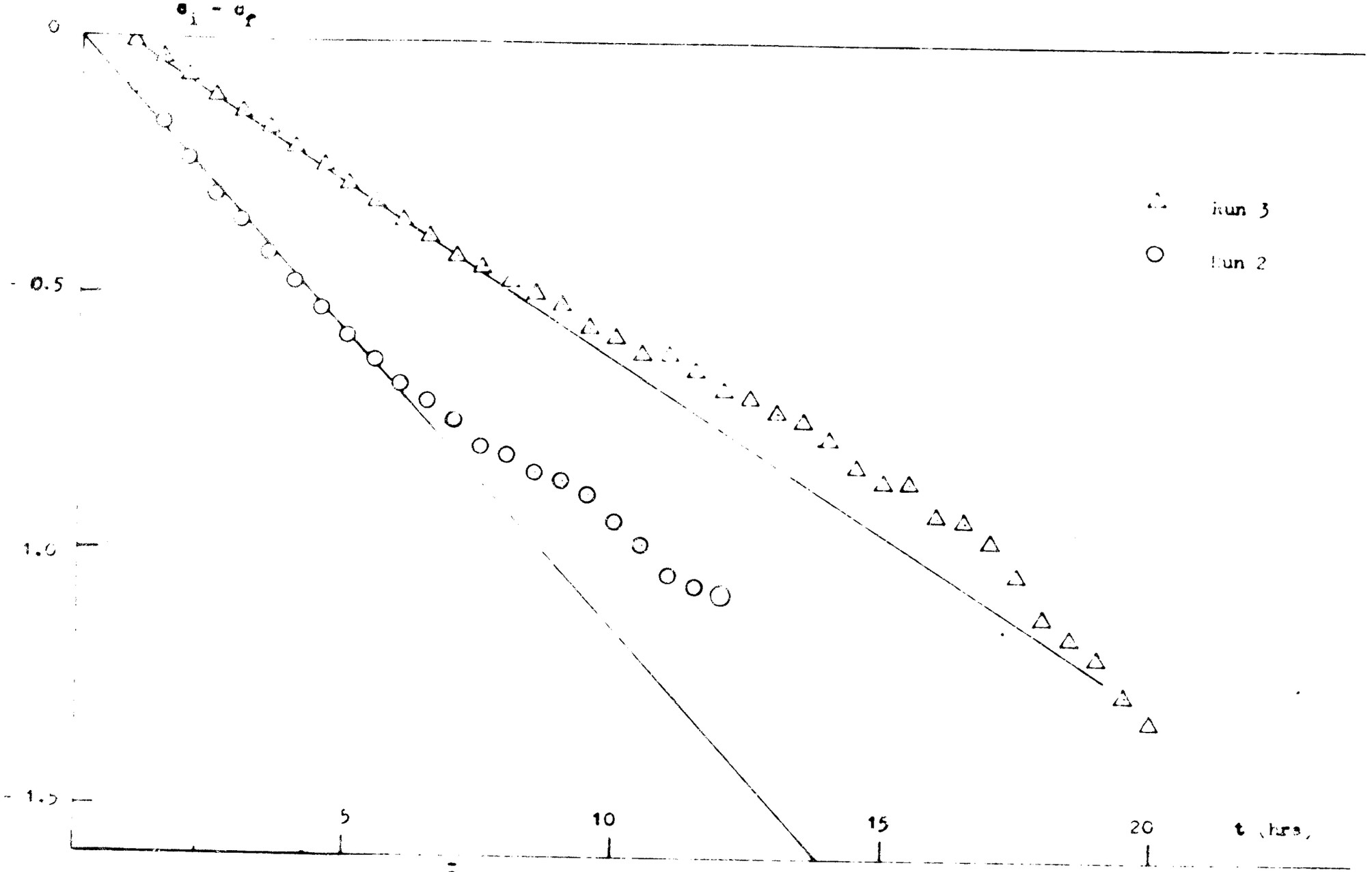

I [illegible]

$\log \frac{c - c_f}{c_i - c_f}$ v time for absorption by Pd08Au12.

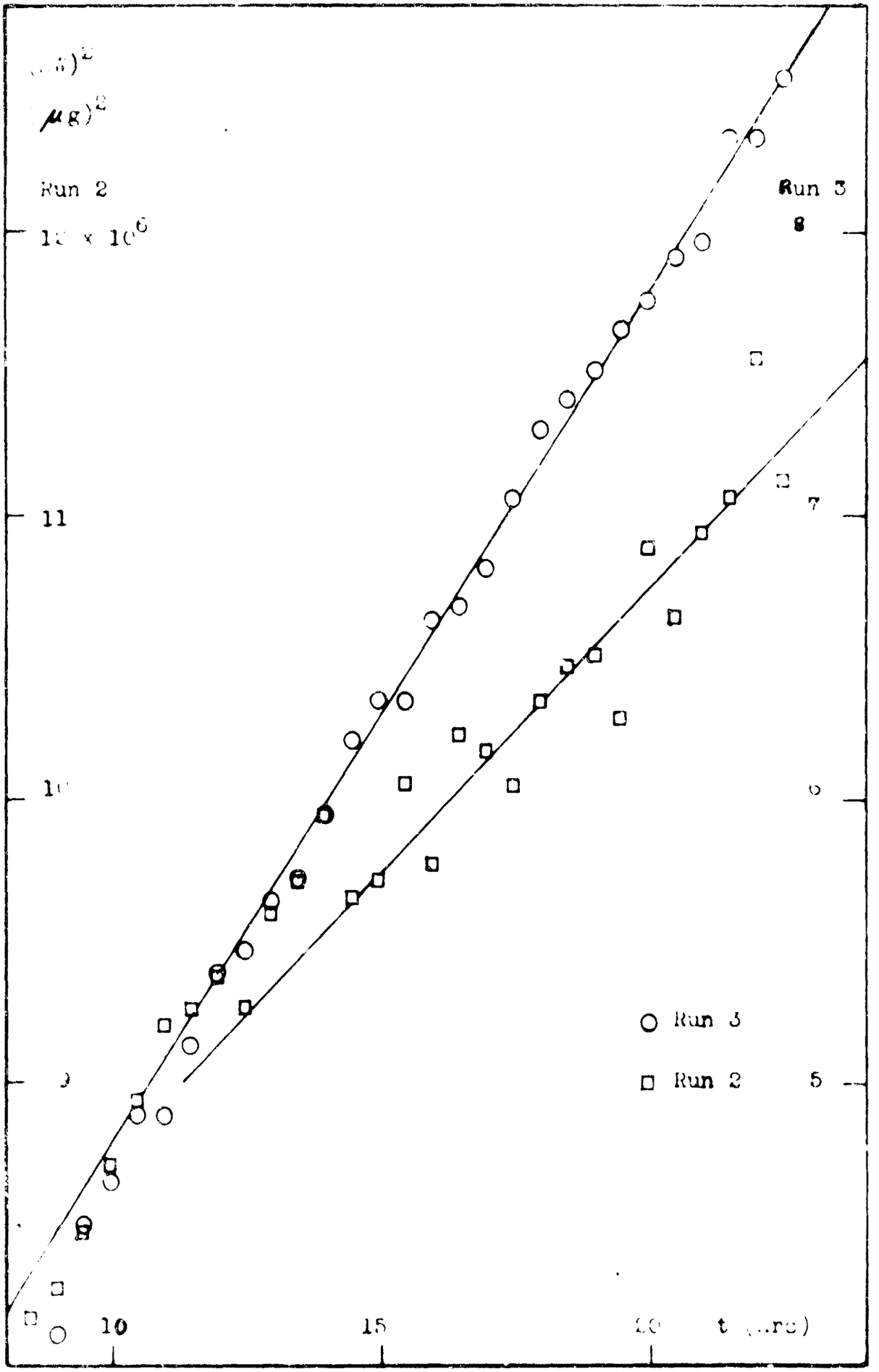

$\Delta\omega)^2$ v time for Pd88Au12.

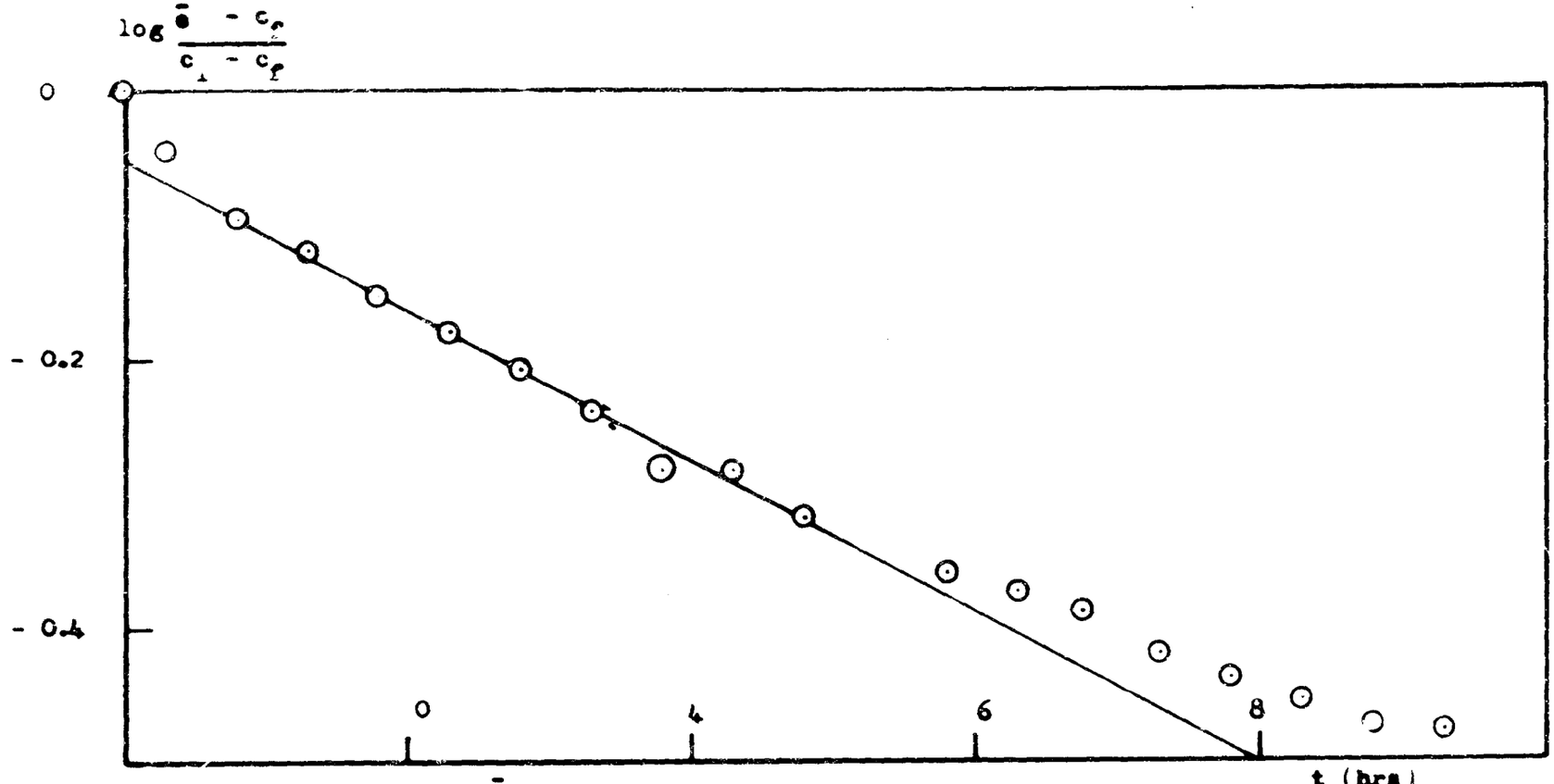

I . 12 $\log \frac{\bar{c} - c_f}{c_i - c_f}$ v time for desorption from Pd69Au31.

TABLE I.1

Results for Palladium - Gold Alloys

Run	Annealing	Cooling (hrs)	Exposure to H(hrs)	Pressure (μ)	α%	p.p.m.H absorbed
		Pd 88 Au 12				
1	800°, 9 hrs	2½	23	½-3½hrs	136 6.5	
				3½-6	Discharge failure	
				6 - 7	137.2 8.5	
				22½-23	138 5.4	3952
2	800°, 3 hrs	2½	23	3½-5	134.4 5.5	
				7-10	139.6 6.8	
				22-23	135.7 8.5	3400
3	790°, 2½ hrs	2½	22½	3 - 4	136.8 3.0	
				5 - 7	137 4.5	
				8 - 9	138.5 4.7	
				22-22½	138.2 6.4	2923
		Pd 69 Au 31				
1	800°, 7 hrs	2½	23	2½-7½	139.5 6.4	
				22½-23	139.7 10.3	1828
2	790°, 6 hrs	2½	23	2½-4½	136.6 12.7	
				22-22½	140 8.8	1746
3	810°, 5 hrs	2½	22½	2 - 8	135 5.1	
				21½-22½	137.5 4.5	1750
		Pd 55 Au 45				
1	800°, 3 hrs	2½				No weight increase
2	790°, 3 hrs	2½	23½	1-10	136.9 9.0	
				22½-23½	137.2 2.7	647

Run	Annealing	Cooling (hrs)	Exposure to H(hrs)	Pressure (μ)			p.p.m.H absorbed
			Pd 55 Au 45 (cont.)				
3	790°, 4 hrs	2½	23	1 -11½	137.8	10.4	
				22½-23½	137.5	8.4	728
			Pd 28 Au 72				
1	780°, 6½ hrs 750°, 2 hrs	2½	23	2½-23½	136.7	12.5	0
2	780 - 800°, 4½ hrs	2½	23½	2½- 8	135	14.7	
				23 -23½	134.7	8.4	0
			Palladium				
1	810°, 6 hrs	2½	23	2½-11	119.7		
				22½-23	125		7185
2	800°, 4½ hrs	2½	35½	3 -11	126.5		
				24	131.5	6.5	
				35½	136.5		6681
3	785°, 3 hrs	2½	22½	2½-6½	128.3		
				22-22½	131.2		6067
4	790°, 7½ hrs	2½	11½	3½-7	114.9		
				8 -9½	119.3		6640
5	790°, 6½ hrs	2½	23½	3 -5½	124.6		
				7 -10	132		
				23-23½	133.2	5	7017
6	790°, 2 hrs	2½	23½	½-7½	137.1		
				22½-23½	138.5		6822

Run	Annealing	Cooling (hrs)	Exposure to H(hrs)	Pressure (μ)		p.p.m.H absorbed
		Gold				
1	800°, 1½ hrs	2	22	¾ - 4	Discharge failure	
				4 - 8	135.7	
				23 -25½	139	0
2	810°, 1½ hrs	2½	47½	9 -10	139.7	
				24½-26½	140.1	
				46½-47½	138.7	0
3	810°, 4 hrs	2½	23	2½- 9½	139.5	
				22½-140	140	0

TABLE I.II

Solubilities of hydrogen in palladium - gold alloys

Alloy	M.Wt.	Run	c H/gm. (p.p.m.)	gm.atoms H/ gm.mol.alloy
Pd	106.4	1	7185	0.764
		2	6681	0.711
		3	6867	0.731
		4	6640	0.706
		5	7017	0.747
		6	6822	0.726
Pd 88 Au 12	117.27	1	3952	0.463
		2	3400	0.399
		3	2923	0.343
Pd 69 Au 31	134.49	1	1828	0.246
		2	1746	0.235
		3	1750	0.235
Pd 55 Au 45	147.17	1	0	0
		2	647	0.095
		3	718	0.106
Pd 28 Au 72	171.63	1	0	0
		2	0	0
Au	197	1	0	0
		2	0	0
		3	0	0

CHAPTER II.

The Oxidation of Metals by Atomic and Molecular Oxygen.

Introduction by R. Heckingbottom and J. W. Linnett.

The present work concerns a study of the oxidation of metals by oxygen atoms and molecules. An R.F. discharge has been used for producing the atoms and the uptake of oxygen by the metals has been determined gravimetrically. The main object has been to determine for which metals the rate and extent of reaction with oxygen atoms differed markedly from that with molecular oxygen. In view of the small amount of previous work on the subject the emphasis has been on conducting a survey of a wide variety of metals, in the hope of detecting some pattern of behaviour.

The oxidation of metals has been, for many years of great interest to the chemist, both for its obvious practical importance and because it has been a fruitful field for testing many ideas based on solid state theory. However, though the effect on oxidation rate due to variation of either the temperature of the system or the composition of both metallic and gaseous phases, has often been studied in detail, that due to dissociation of the attacking gas has received relatively little attention.

It was felt that further work in this latter field was desirable for two main reasons. Firstly where work of this kind has been attempted the effect of atoms has sometimes been shown to be considerable. Secondly as interest in the upper atmosphere - a region where a relatively high proportion of molecules are dissociated or excited - increases, the subject grows in technological importance.

Previous work with dissociated or activated oxygen.

The most marked contrast in behaviour, towards oxygen atoms on the one hand and molecules on the other, is shown by silver.

In a recent detailed survey, Czanderna (J. Phys. Chem. 68, 2765, (1964)) has shown that between -77°C and 351°C oxygen is chemisorbed on silver, probably as O^-, O_2^- and O_2, but that coverage never exceeds a monolayer. This confirms earlier work and the oxidation of silver by molecular oxygen has only once been reported (Menzel and Menzel-Kopp, Surface Science 2, 376, (1964)), when crystallities of Ag_2O were observed on silver at 250°C under 35 atmospheres of oxygen.

In contrast, several workers have observed the oxidation of silver by oxygen atoms even at room temperature (e.g. Linnett and Marsden, Fifth Int. Symp. Combustion, 685, (1955)). Silver probes have in fact been used to give a measure of atom concentration (Jennings Quart Rev. 15, 237, (1961)), these probes being quickly blackened due to oxide formation. However, there has been only one previous investigation of the kinetics of the reaction (Tyapkina and Dankow, Doklady Akad. Nauk. S.S.S.R. 59, 1313 (1948)). Even here observations were limited to the first twenty minutes of reaction; the uptake was found to follow the parabolic rate law approximately.

Several workers have found that the presence of oxygen atoms increases the rate of oxidation if the oxide formed is volatile. Rossner and Allendorf (J Chem. Phys. 40, 3441, (1964)) have found that between 800 °C and 1300°C atoms increase the rate of oxidation of molybdenum by a factor of about twenty - MoO_3, the main product, is volatile at these temperatures. Similarly, Fryburg (J. Chem. Phys. 24, 175, (1956)) has shown that platinum is oxidised to volatile PtO_2 at 1,000°C and that oxygen atoms are up to four hundred times as effective as molecules. Further, Sutcliffe (D.Phil. Thesis, Oxford (1964)) reports

that atoms greatly increase the oxidation rate of chromium above 150°C due to the formation of CrO_3 which is volatile above this temperature

According to Dravnieks (J. Amer. Chem. Soc., 72, 3761, (1950)), the effect of oxygen atoms on the oxidation of copper is complex due largely to the fact both Cu_2O and CuO may be present in the oxide scale. Atoms tend to increase the rate of oxidation during the initial period when only Cu_2O is formed and also to shorten this period. When both oxides were present, atoms had little effect.

A little oxidation work has also been carried out using oxygen activated by a tesla coil, notably by Leibowitz et al. (J. Electrochem. Soc. 108, 1166, (1961)) who found that the rate of oxidation of uranium to the non-protective UO_2 was increased by up to twenty fold on switching on the coil.

In addition several workers e.g. Hauffe and Engel (Z. Electrochem. 57, 773 (1953)) and Dickens and Sutcliffe (Trans. Faraday Soc., 60, 1272 (1964)), have shown that the presence of activated or dissociated oxygen increases both the amount of chemisorbed oxygen and the conductivity of several oxides. Thus in the case of a growing oxide these changes in the surface concentration may well alter the concentration gradients in the bulk and hence influence the oxidation rate. Previous to the present work however there appears to have been no attempt to relate the effects of atoms to the general oxidation theory proposed by Wagner.

Experimental.

The experimental method may be outlined as follows. A controlled supply of oxygen flows first through an RF discharge, resulting in partial dissociation of the gas, and then past the open end of a vertical

side arm. The latter is closed at its upper end so that there is no net flow along it; atoms diffuse into the tube under a concentration gradient. The sample, suspended from the arm of a microbalance, is situated in the vertical side arm and its oxidation is followed gravimetrically. In addition the side arm could be heated so that oxidations could be studied at any temperature between 25°C and 800°C. This appears to be the first apparatus to be used that combines the continuous production of atoms with the direct gravimetric investigation of oxidation.

The oxygen was produced electrolytically and used in its undried state as the presence of about 2% water vapour increases the degree of dissociation of oxygen in the RF discharge from about 2% to 10%. The operating pressure was about 1.0 microns, the gas flow being controlled by a thermostated needle valve. Pirani gauges were used for pressure measurement at normal operating pressures, and pressure of around 10^{-5} mm used in outgassing procedures were recorded on a Penning gauge.

The sample was suspended by a quartz fibre from one arm of a Sartorius microbalance. This balance was capable of detecting changes of ± 1 µg or greater and total weight changes up to 10^4 µg could be followed. Samples weighing up to 1 g could be used, the greater part of the load being off set by counterweights.

The vertical diffusion arm was heated by a nichrome wire furnace wound onto its outside, and the sample temperature during runs was measured by a thermocouple on the furnace wall, previously calibrated against a second thermocouple placed in the normal sample position. The temperature could be maintained within ± 2°C of any desired value between 25°C and 800°C. Baffling and a cooling fan were introduced to protect the balance head from

the furnace region; the discharge tube was also fan cooled.

Atom concentrations were determined with silver tipped thermocouple probes and thus only a relative measure was obtained. However comparison with earlier work on similar systems, using both probes and Wrede gauges (Linnett and Greaves, Trans. Faraday Soc. 54, 1323, (1958)), suggested that the atom concentration in the sample region was equivalent to a pressure of 6 μ at room temperature. Unfortunately at higher temperatures the silica walls of the surface became much more active towards atom recombination and the atom concentration in the sample region may fall to as low as 10^{-3} μ by 750°C.

One probe was placed in a small side arm just downstream of the discharge tube, to monitor the atom concentration during runs. A second similar probe, tipped with the metal under investigation could also be introduced, by means of a side arm in the furnace, into the normal (but vacant) sample position. The purpose of this was twofold; first the probe was used to check the relative atom concentrations under various conditions and second, as the sample temperature rises in the presence of atoms just as that of a probe does, the magnitude of this rise is required for each metal. Thus so that the sample temperature would be the same for runs with and without the discharge on, the furnace wall temperature was set at an appropriately lower temperature in the latter case.

Although this corrects for the the temperature effect due to atoms over the greater part of a run, it still leaves the problem of the initial temperature rise on switching the discharge on. The effect is small at say 500°C as the total change is only about 3°C, but at 150°C

the temperature rise is about 15°C occurring over the first five minutes of the run, and this must be borne in mind when analysing the results quantitatively.

One further correction was necessary, as the thermomolecular effects were large at the operating pressure. Fortunately if the sample was brought to temperature under a vacuum of 10^{-5} mm or better and the oxygen was then introduced the thermomolecular effect registered immediately and hence could readily determined.

The metal samples were normally prepared as follows:- a) abrasion with a fine grade emery paper, b) rinsing with carbon tetrachloride c) drying in a current of warm air and d) outgassing at 700°C and 10^{-5}mm. for 30 minutes. In the case of zirconium, process a) was replaced by a chemical polish in a solution containing 45% H_2O, 45% conc HNO_3 and 10% HF. Zinc and cadmium could not be outgassed as in d) due to their high vapour pressures, this stage was also omitted in the case of tin foil oxidation due to its low melting point.

Results.

The fourteen metals:- nickel, cobalt, iron, silver, copper, zirconium, aluminium, tantalum, tin, zinc, cadmium, palladium, platinum and gold, have been studied. The main results will now be given metal by metal.

Nickel.

All the oxidations showed a parabolic time dependence and the presence of atoms increased the rate constant considerably in all cases as shown in Table 1.

TABLE 1.

The Oxidation of Nickel.

Run	Temperature °C	Gas phase species	k_{p_4} $gm^2./cm^4/sec$
1a	428	O_2	$4.53 \cdot 10^{-16}$
1b	430	$O + O_2$	$1.53 \cdot 10^{-14}$
1c	545	O_2	$1.21 \cdot 10^{-13}$
1d	545	$O + O_2$	$7.28 \cdot 10^{-13}$
2	494	O_2	$2.45 \cdot 10^{-14}$
4	490	$O + O_2$	$2.13 \cdot 10^{-13}$
3	648	O_2	$3.08 \cdot 10^{-13}$
5	650	$O + O_2$	$4.38 \cdot 10^{-12}$

The results of runs 1a, 1b, 1c and 1d are shown in Fig. II.1. The ratio k_p (atoms)/k_p(molecules) was about 10 at 600°C and some what higher at lower temperatures, the activation for oxidation being 38 kcal./mole in the presence of molecules and 33 kcal/mole in the presence of atoms: only four points were available for determining each figure however. The grey black scale was considered to be NiO.

Cobalt.

The oxidations again followed a parabolic time law. At lower temperatures (below about 660°C) atoms caused only a slight increase in the rate but at higher temperatures (about 700°C) a marked increase resulted, the ratio k_p (atoms/k_p(molecules) being about 6. This is borne out by the results in table 2 and confirmed in a qualitative manner by the results of successive runs on sample 1 as shown in fig. II.2

TABLE 2.

The Oxidation of Cobalt.

Run	Temperature °C	Gas phase species	k_p $gm^2./cm^4/sec$
2	564	0_2	$8.46 \cdot 10^{-12}$
3	563	$0 + 0_2$	$1.00 \cdot 10^{-11}$
4	713	0_2	$1.02 \cdot 10^{-11}$
5	713	$0 + 0_2$	$6.12 \cdot 10^{-11}$
1e	713	0_2	$1.23 \cdot 10^{-11}$
1f	714	$0 + 0_2$	$7.21 \cdot 10^{-11}$

At the lower temperature (runs 2 and 3) both CoO and Co_3O_4 were present in the scale, at the higher temperature only CoO was found. Investigation of the thermal decomposition of the scale formed in runs 2 and 3 showed that the Co_3O_4 content was about 31% by volume in each case.

Iron.

When single runs were carried out on samples the parabolic rate law was followed and atoms had no detectable effect, as shown in Table 3.

TABLE 3.

Run	Temperature °C	Gas phase species	k_p $gm^2./cm^4/sec$
3	652	0_2	$1.61 \cdot 10^{-9}$
4	651	$0 + 0_2$	$1.61 \cdot 10^{-9}$
5	652	$0 + 0_2$	$1.69 \cdot 10^{-9}$

Further runs at 227°C, 495°C and 563°C confirmed that atoms had no effect. Data from these runs were not analysed quantitatively however as

several runs were carried out on the same sample leading to deviations from the parabolic law. Above about 570°C the bulk of the scale was assumed to be mainly non-stoichiometric FeO with successive layers of Fe_3O_4 and Fe_2O_3 outside it, below 570°C the FeO layer is known to disappear or to remain only as a thin subscale on top of the metal.

Silver.

The results of oxidising silver by atomic oxygen are shown in table 4.

TABLE 4.

The Oxidation of Silver.

Run	Temperature °C	k_{p_4} $gm^2/cm.^4/sec$	k_{c_4} $gm.^2./cm^4/sec$
1f	277	$5.81 \cdot 10^{-11}$	
1g	225		$1.45 \cdot 10^{-14}$
1h	168		$1.82 \cdot 10^{-15}$
1i	310	$1.52 \cdot 10^{-10}$	
1j	65	$1.10 \cdot 10^{-11}$	
2b	65?	$5.53 \cdot 10^{-12}$	

Thus, in the main, the oxidation follows a parabolic rate law with deviations towards cubic in some instances, see Fig. II.3. The majority of runs were carried out on the same sample as the silver was regenerated between runs by heating the oxide to above 350°C at 10^{-5} mm. The oxidation rate is seen to be remarkably fast for such low temperatures (c.f. k_p for Co or Ni at 600°C - 700°C) this being largely due to the low temperature coefficient for the process determined here as 10 ± 3.5 kcal/mole for the temperature range 170°C to 310°C. Below 170°C the rate is even faster than would be expected from an extrapolation of the higher temperature

results. Above 170°C only Ag_2O appears in the scale but at room temperature both Ag_2O and an outer layer of AgO are present, about 40% of the oxygen being in the latter.

Copper.

The results obtained for copper fall into two groups - below 250°C where only thin oxide films are formed and above 400°C where thick films are obtained. The thin film region will be considered first. With O_2 the uptake was too small for the data to be analysed accurately. In the presence of atoms the uptake was increased by a factor of about seven. Earlier work (e.g. by Gwathmey et. al. Acta Metallurgia 4, 145, 153, (1956)) has shown that the rate of oxidation depends on the crystal face exposed; the rate with atoms is five or six times faster than the fastest rate observed with O_2. Initially at about 150°C the uptake followed a logarithmic law but the later stages of the runs could also be represented by a cubic plot. The range of applicability of the cubic law increased with temperature extending over a complete run by 200°C. The cubic rate constants were:-

Temperature °C	k_c gm.^{3}/cm.^{6}/sec
140	$3.52 \cdot 10^{-19}$
163	$1.12 \cdot 10^{-18}$
213	$8.73 \cdot 10^{-18}$

and the activation energy was 18 kcal./mole. The scale was blackish indicating that it was mostly CuO.

Above 400°C the oxidation behaviour was somewhat more complex. In molecular oxygen at 40 μ the rate was linear e.g. at 453°C,

$k_p = 9.33 \cdot 10^{-9}$ gm./cm.^{2}/sec., but at 19.2 cm pressure of O_2 the rate was parabolic, ($k_p = 2.77 \cdot 10^{-11}$ g.m.^{2}/cm.^{4}/sec.) comparing well with rates observed by other workers at similar pressures (e.g. Valenci Rev. Metall 45, 10, (1948)). The linear rate constant increased almost linearly with pressure (see Fig. II.4 for sample 6 at 575°C) until by the time the pressure reached 0.5 mm. diffusion through the scale became rate determining and the parabolic rate law was followed.

In comparison, only a short linear period was observed in the presence of atoms and at comparable temperatures and pressures the rate constant is about fifteen times greater than with O_2. Subsequently parabolic law is followed, k_p being comparable with that obtained with high pressures of O_2, see Fig. II.4. The activation energy of 20.7 kcal/mole from the parabolic rate constants is in good agreement with Valenci's value of 20.1 kcal./mole. The scale was again predominantly CuO though it was probable that, in the initial periods when the linear rate was observed, only Cu_2O was present. (Honjo, J. Phys. Soc. Jap. 4, 330, (1949)).

Zirconium.

The results obtained for the oxidation of zirconium are shown in table 5.

TABLE 5.

The Oxidation of Zirconium.

Run	Temperature °C	Gas phase species	k_p $gm^2/cm^4/sec$	k_c $gm^2/cm^6/sec$
2a	518	O_2	$6.28 \cdot 10^{-13}$	
2b	520	$O + O_2$	$9.62 \cdot 10^{-13}$	
2c	636	O_2	$1.62 \cdot 10^{-11}$	
2d	637	$O + O_2$	$2.41 \cdot 10^{-11}$	
6a	435	O_2	$4.00 \cdot 10^{-14}$	
6b	435	$O + O_2$	$4.33 \cdot 10^{-14}$	
7	498	$O + O_2$	$5.28 \cdot 10^{-13}$	
8	496	O_2		$6.10 \cdot 10^{-17}$
3	535	$O + O_2$	$1.71 \cdot 10^{-12}$	
4	535	$O + O_2$	$1.50 \cdot 10^{-12}$	
5	535	O_2		$4.18 \cdot 10^{-17}$

A mean squares analysis of the k_p values gave activation energies of 38.4 kcal./mole and 38.8 kcal./mole for molecules and atoms respectively; the plots are shown in Fig. II.5. The presence of atoms increased the oxidation rate slightly e.g. at 560°C k_p (atoms)/k_p(molecules) = 1.46.

Other metals.

The results for the other metals will now be considered more briefly.

Aluminium.

The introduction of atoms appeared to have no effect on the oxidation rate in the temperature range 25 °C to 660°C (the melting point of aluminium).

Tantalum.

Atoms again appeared to have little effect when the scale was protective, the results were somewhat irreproducible however as the protectiveness of the scale varied. In some runs, where the rate of uptake was almost linear both the presence of atoms and higher pressures of O_2 increased the rate.

Tin.

The effect of atoms on the oxidation of tin foil (below 232°C) was small and was too small to be detected in the case of oxidation of liquid tin. In the latter case the scale again afforded a variable degree of protection.

Zinc and Cadmium.

Investigations were only carried out in the temperature range 25°C to 150°C, due to the high vapour pressure of the metals. No oxidation was detectable in the presence of either atomic or molecular oxygen.

Palladium.

Only thin oxide films formed on palladium at the higher temperatures (above 550°C) where, at atmospheric pressures, a thick oxide film results, the oxide decomposed at the low operating pressures used in the present work. The uptake in all temperature range 350°C to 450°C was approximately logarithmic but induction periods were observed initially. Atoms tended to eliminate these induction periods but did not cause any increase in the total uptake.

Platinum and Gold.

Neither of these metals were oxidised to any detectable extent by either atomic or molecular oxygen, in the temperature range 25°C to 500°C.

Discussion.

Nickel.

When nickel is oxidised it forms a scale consisting of the single p-type oxide, NiO. According to the Wagner model the scale grows as a result of transport of fresh metal to the gas oxide interface under a concentration gradient of nickel ion vacancies, $Ni^{2+}\square$. At the metal/oxide interface the $Ni^{2+}\square$ concentration is almost zero but at the gas/oxide interface it is much larger due to the reaction

$$2Ni^{2+} + \tfrac{1}{2}O_2 = NiO + Ni^{2+}\square + 2Ni^{3+}, \quad \Delta\bar{G}_1^o \qquad \text{------(1)}$$

(when the gas is O_2), All charged species are on the cation sub-lattice in NiO, $\Delta\bar{G}_1^o$ is the partial molal standard free energy of reaction (1).

Applying the law of mass action

$$(Ni^{2+}\square)\,(Ni^{3+})^2 = PO_2^{\frac{1}{2}} \exp\,(-\Delta\bar{G}_1^o/RT)$$

assuming that concentrations are equal to activities and, that (Ni^{2+}) and (NiO) are constant. Thus from (1) $(Ni^{2+}\square) = \frac{1}{2}(Ni^{3+})$ and

$$(Ni^{2+}\square) = 4^{-\frac{1}{3}}\, PO_2^{\frac{1}{6}} \exp\,(-\Delta\bar{G}_1^o/3RT) \qquad (1a)$$

When atoms are present the analogue of reaction (1) is

$$2Ni^{2+} + O = NiO + Ni^{2+}\square + 2Ni^{3+}, \quad \Delta\bar{G}_2^o \qquad \text{------(2)}$$

and by similar analysis

$$(Ni^{2+}\square) = 4^{-\frac{1}{3}}\, PO^{\frac{1}{3}} \exp\,(-\Delta\bar{G}_2^o/3RT) \qquad (2a).$$

Thus the vacancy concentration is more sensitive to the pressure of atoms. More important, however is the difference between $\Delta\bar{G}_1^o$ and $\Delta\bar{G}_2^o$ - subtraction of (2) from (1) gives

$$\tfrac{1}{2}O_2 = O \qquad \Delta\bar{G}_1^o - \Delta\bar{G}_2^o = \Delta\bar{G}_d^o,$$

hence (2a) becomes

$$(Ni^{2+}\square) = 4^{-\frac{1}{3}}\, PO^{\frac{1}{3}} \exp\,(-\Delta\bar{G}_1^o/3RT) \exp\,(\Delta\bar{G}_d^o/3RT)$$

As $\Delta\bar{G}_1^o$ is positive, at comparable pressures, atoms lead to far more vacancies in the scale, near the gas/oxide interface, than do molecules the concentration

gradient across the scale rises by almost the same factor.

At 650°C and 40 μ pressure PO_2 in atmospheres is about 5.10^{-5}, PO, when the discharge is on, is about 10^{-3} and under these conditions the rates (Ni^{2+} □) (atoms)/(Ni^{2+} □) (molecules) is 11.13 in very good agreement with the observed value of 10.

The oxidation rate depends on the product of the concentration and the mobility of the nickel vacancies. Hence, in the presence of O_2, the activation energy for oxidation is $(\Delta \bar{H}_1^o/3 + V)$ where $\Delta \bar{H}_1^o$, is the standard heat of reaction (1) and V is the activation energy for diffusion of the vacancy. When atoms are present the activation energy becomes $(\Delta \bar{H}_2^o/3 + V)$ where $\Delta \bar{H}_2^o = \Delta \bar{H}_1^o - \Delta H_d^o$. ΔH_d^o is about 59 kcal/mole so that the presence of atoms should lower the activation energy by nearly 20 kcal/mole.

In fact the activation energy in the presence of O was only about 5 kcal lower than in the presence of O_2. Most of this discrepancy may be attributed to a trace of iron impurity shown by spectrographic analysis to be present to the extent of about 1ppm. This is sufficient to explain the rather high values of k_p at $PO_2 = 5.10^{-5}$ and as the iron has most effect at the lower temperatures the slightly low value for the activation energy. Further it will reduce the observed effect due to atoms again in the low temperature range as compared with that predicted for pure nickel.

Cobalt.

At the higher temperatures where only CoO is formed, the situation is similar to that discussed for NiO and atoms cause a large change in the k_p value. Slight numerical differences occur because of increased association of defects in the scale i.e. the analogue of reaction (1) is

$$2Co^{2+} + \tfrac{1}{2}O_2 = CoO + (Co^{2+} \ldots Co^{3+}) + Co^{3+}$$

and the concentration of complexed vacancies is $PO_2^{\frac{1}{2}}$; in the presence of atoms it accordingly becomes $PO^{\frac{1}{2}}$.

The main discrepancy between theory and practice arises from the fact that an outer layer of Co_3O_4 should still be thermodynamically stable at 700°C in the presence of atoms but none could be detected. Two factors may account for this:- at these temperatures the arrival rate of atoms is no longer much greater than the incorporation rate of oxygen by the scale and this may lead to non-equilibrium conditions at the surface, further, as with silver and palladium, it was found that the critical temperature at which an oxide became unstable in the presence of atoms was that at which its decomposition rate, in the presence of O_2, became very rapid, again suggesting that kinetic factors were playing an important role.

At the lower temperatures, the bulk of the scale is still CoO and as it is bounded by the Co/CoO and the CoO/Co_3O_4 interfaces its growth rate is largely independent of changes in the oxygen potential in the gas phase. Thus theory predicts that the presence of atoms will affect only the minor constituent in the scale and their effect will be small. The final prediction is correct but there was no evidence that the Co_3O_4 content had increased.

Iron.

The absence of any effects due to atoms is in complete agreement with the predictions of theory. Any FeO in the scale (it is the major constituent above about 570°C) grows between the Fe/FeO and the FeO/Fe_3O_4 interfaces and is not affected by atoms in the gas phase. Similarly Fe_3O_4 (a major constituent below 570°C) grows between the FeO/Fe_3O_4 and the Fe_3O_4/Fe_2O_3 interfaces. Finally the outer layer of Fe_2O_3 is n-type and its growth rate is virtually independent of the oxygen potential in the gas

phase - this point will be considered in greater detail in the section on n-type oxides.

Silver.

In the review of previous work it was pointed out that oxygen is chemisorbed on silver up to 310°C. The present work shows clearly that it is not diffusion rates in the solids that prevents this oxygen forming an oxide scale. Thus it must be that molecular oxygen is not dissociatively adsorbed on the silver at temperatures below which the oxides of silver are stable (185°C for Ag_2O when $PO_2 = 1$).

The low activation energy for oxidation is in keeping with the low activation energy for ionic conduction and diffusion in several other silver salts. As Ag_2O is a p-type oxide the high rate of oxidation observed at 65°C will, at least in part, be due to the considerable increase in PO with the reduction in temperature. The situation is complicated by the formation of an outer layer of AgO, containing nearly 40% of the total oxygen uptake. Unfortunately a rigorous analysis of the results is not possible as the stability range of the AgO appears to be governed by kinetic rather than thermodynamic factors.

Copper.

In the low temperature region the increase in uptake due to atoms may well be caused by an increase in the amount of dissociated oxygen adsorbed on the surface as in the case of silver. Following charge transfer this will lead to a stronger field across the film leading to increased uptake at faster rates as observed.

At higher temperatures and low pressures of O_2 the diffusion through the oxide is faster than the reaction at the gas/oxide interface.

Thus increasing the oxygen potential in the gas phase, either by increasing the pressure of O_2 or by introducing atoms, causes a large increase in the oxidation rate. When the extent of oxidation is large however, both CuO and Cu_2O are present in the scale and the effect of atoms or of variation in PO_2 is small.

Metals Oxidising to form *n*-type oxides.

This group includes the metals Zr, Al, Zn, Cd, Ta and Sn. In the oxidation of zirconium, the ZrO_2 scale grows at the Zr/ZrO_2 interface following transport of fresh oxygen through the scale by means of anion vacancies. The concentration of these vacancies is large at the metal/oxide interface and virtually zero, even in the presence of O_2, at the gas oxide interface. Thus the presence of atoms in the gas phase only brings the lower concentration even closer to zero and their effect is consequently negligible. Similarly the supply of interstitial zinc responsible for the transport of fresh material across a growing scale of ZnO on Zn is governed almost entirely by the Zn/ZnO interface reactions.

In the cases where the scale remained protective this predicted behaviour was in general observed for the metals investigated in this work. The small but definite increase in k_p values, due to atoms, observed for zirconium is probably connected with the surface preparation. Gulbransen and Andrew (J. Metals 9, 394, (1957)) have shown that after an electrochemical polish the rate of oxidation of zirconium is slower and more likely to follow the parabolic time law than after abrasion. The results presented here confirm the predominance of the parabolic rate law after this preparation and the k_p values for O_2 are in good

agreement with Gulbransen's. The effect of atoms is rather less than that of abrasion; both probably influence the subscale formed at the metal oxide interface, the bulk of the scale behaving as predicted by the theoretical model.

Palladium, platinum and gold.

The results for palladium oxidation support the idea that the initial nucleation and growth of the oxide are speeded by the greater abdundance of O or O^- on the surface resulting from the presence of atoms in the gas phase. Again the presence of atoms did not increase the temperature range over which the PdO was stable as would be expected on thermodynamic grounds. The inactivity of gold and platinum in the presence of oxygen appears to be due to a property of the metals, possibly connected with their high first ionisation potentials, and does not depend on the state of the oxygen as is found for silver.

Conclusions.

The survey has shown that the effect of oxygen atoms in the gas phase, on the oxidation of a wide range of metals, can be explained in a semiquantitative manner by the existing theories of oxidation. Maximum effects were found as predicted, when the scale consisted of a single p-type oxide such as NiO and very small effects resulted when an n-type oxide such as ZrO_2 or a multi-oxide scale such as $FeO/Fe_3O_4/Fe_2O_3$ was formed. Further work with oxides like NiO in conjunction with a more abundant and variable, known atom concentration would provide a more rigorous test of theory, as the pressure dependence and activation energy in the presence of atoms could then be determined accurately.

The work on silver suggests that in this case it is the absence of dissociative adsorption of O_2 that prevents oxidation in molecular oxygen. Here, as with cobalt, further work with large known atom concentrations should provide more information about the interesting problem of the stability of higher oxides in the presence of atomic oxygen.

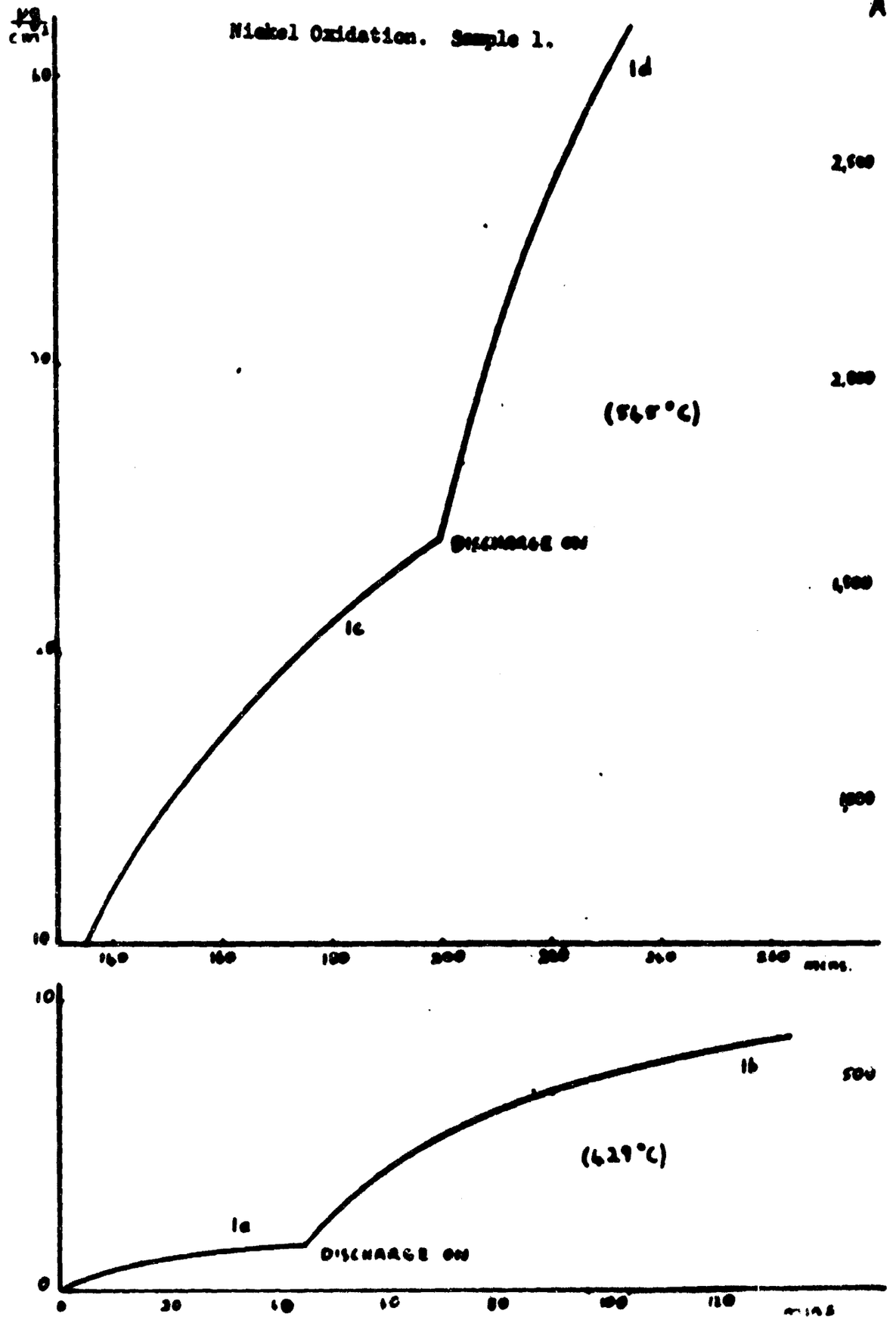

Fig. II.1.

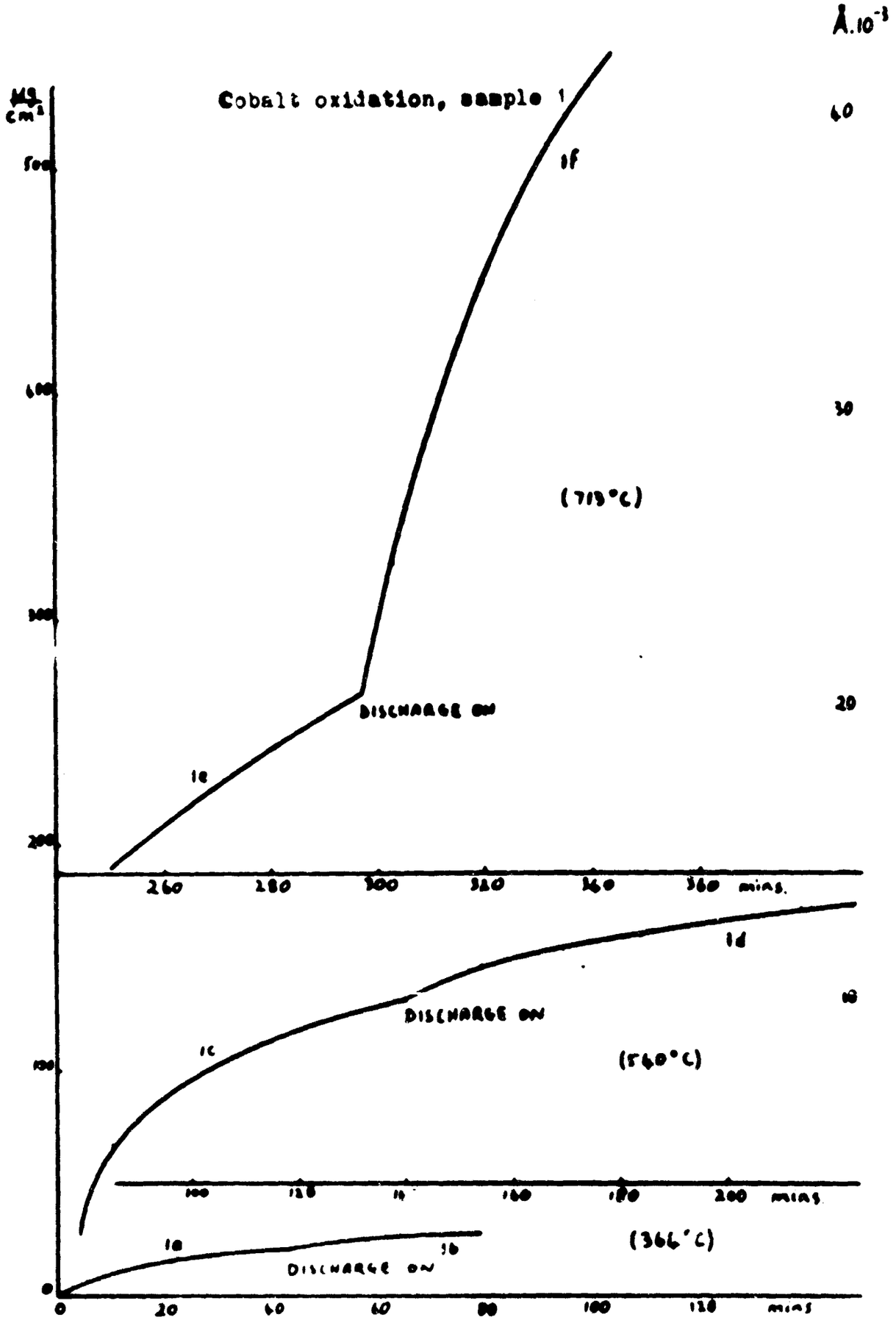
Cobalt oxidation, sample 1
Å.10⁻³
mg/cm²
60
30
20
10
0
1f
1e
1d
1c
1b
1a
DISCHARGE ON
DISCHARGE ON
DISCHARGE ON
(719°C)
(560°C)
(366°C)
240 280 300 320 340 360 mins.
100 120 140 160 180 200 mins
0 20 40 60 80 100 120 mins

Fig. II. 2

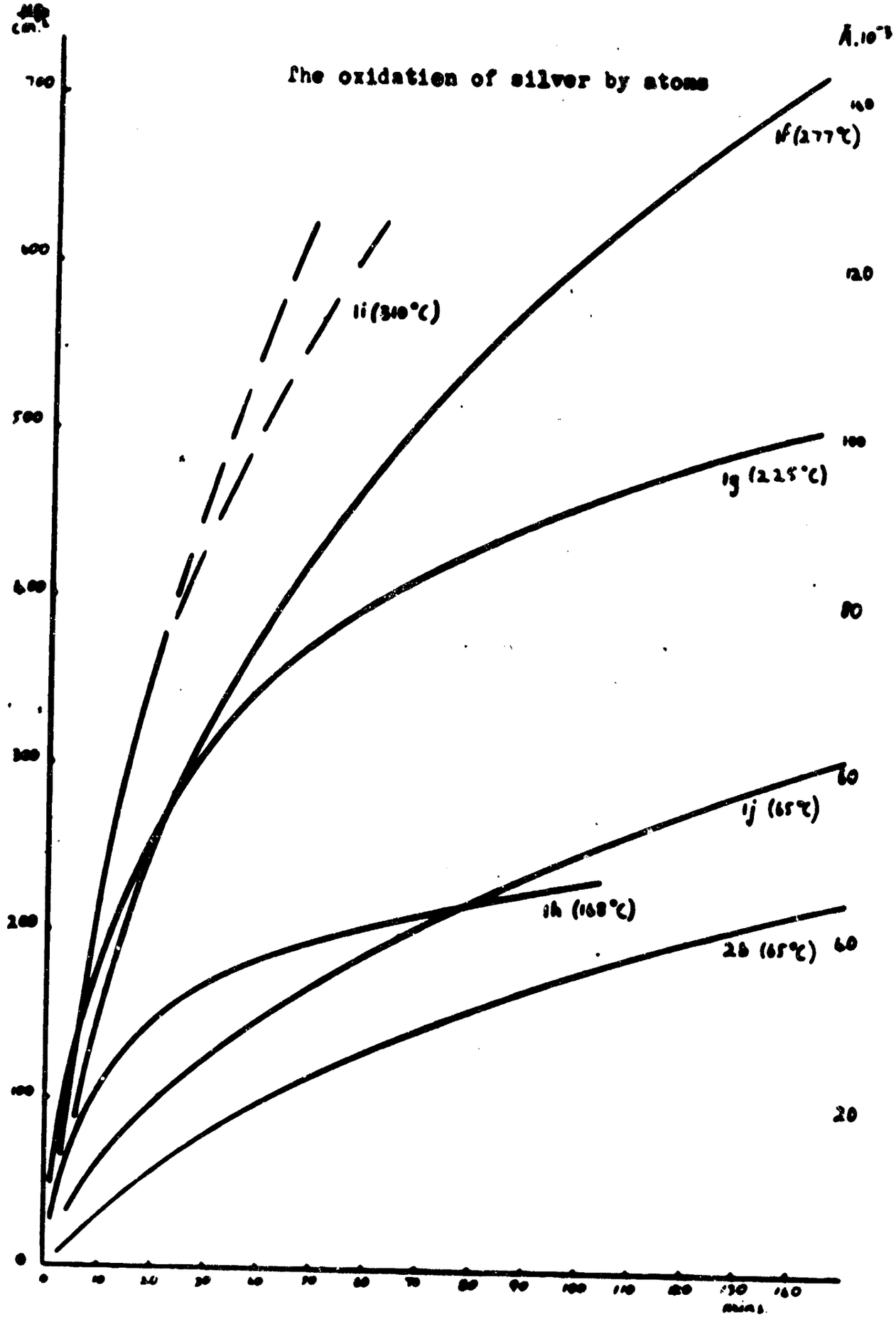
Å.10⁻¹
700
600
500
400
300
200
100
0
140
120
100
80
60
40
20
If (277°C)
Ii (340°C)
Ig (225°C)
Ij (65°C)
Ih (168°C)
2b (65°C)
0
10
20
30
40
50
60
70
80
90
100
110
120
130
140
mins.

Fig. II. 3.

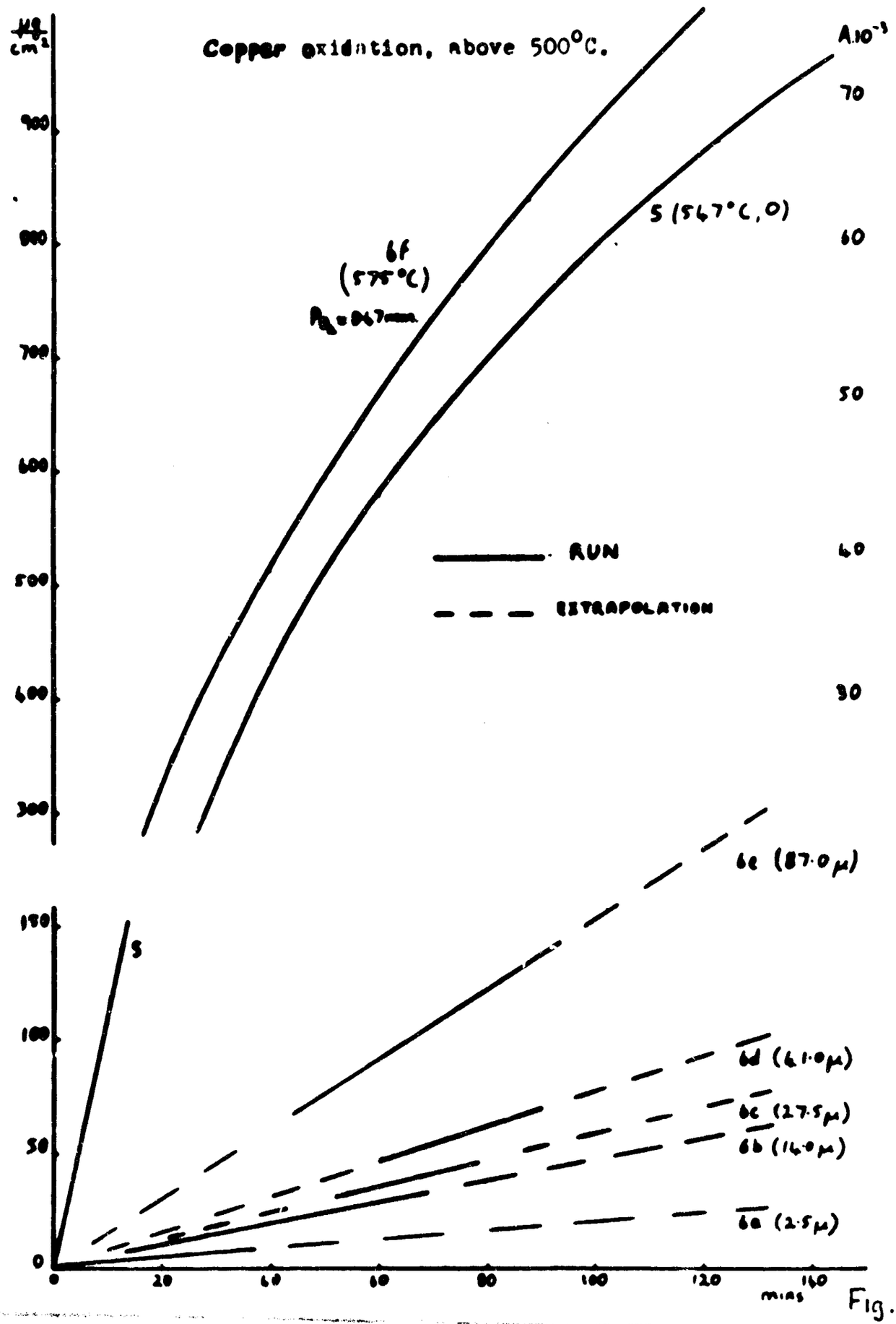
Copper oxidation, above 500°C.
μg/cm²
A.10⁻³
900
800
700
600
500
400
300
70
60
50
40
30
δf (575°C)
S (567°C, O)
RUN
EXTRAPOLATION
δe (87.0μ)
δd (61.0μ)
δc (27.5μ)
δb (16.0μ)
δa (2.5μ)
S
150
100
50
0
0
20
40
60
80
100
120
140
mins

Fig. II 4

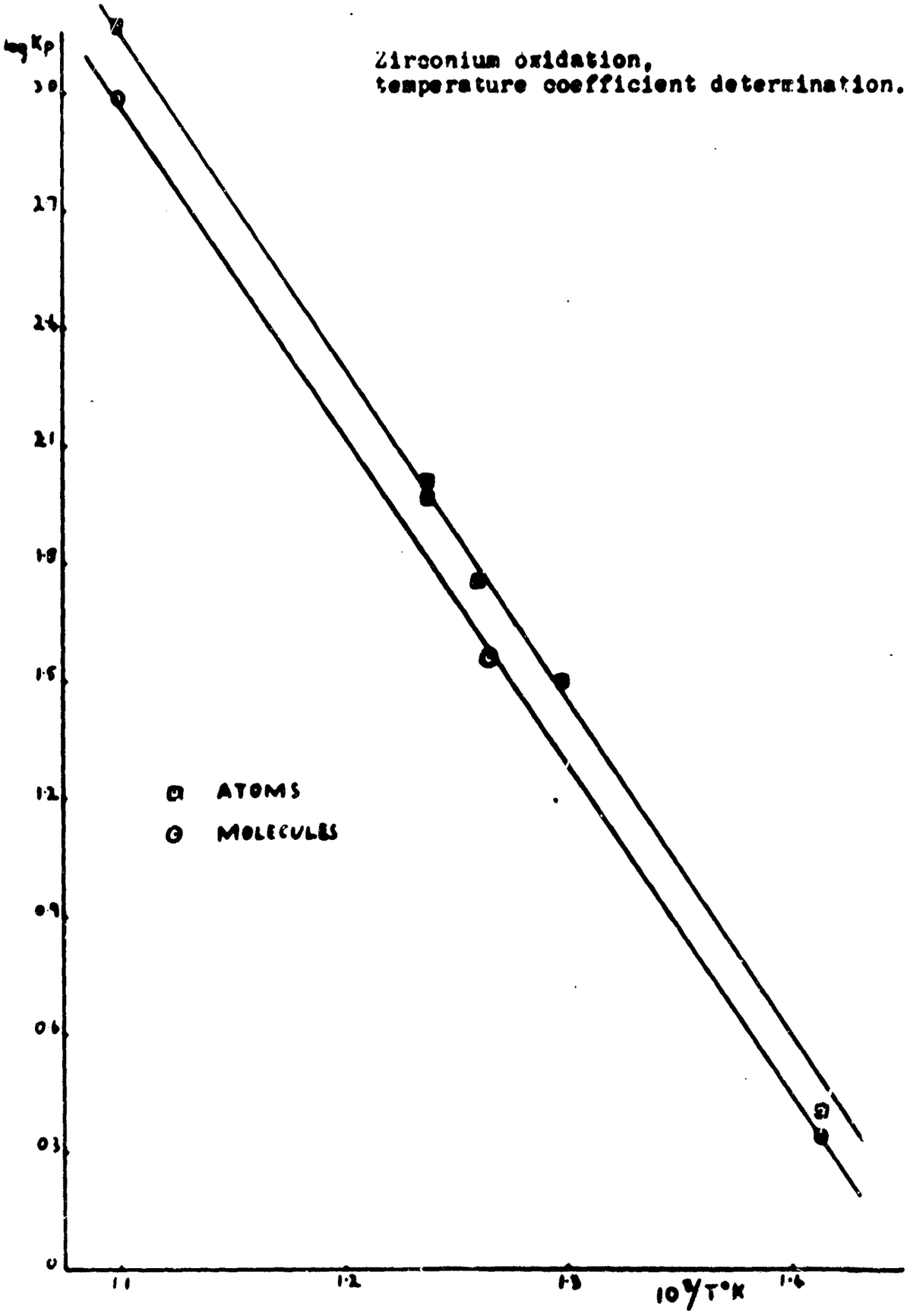
Zirconium oxidation,
temperature coefficient determination.
log Kp
2·0
1·7
1·4
1·1
0·8
0·5
0·2
0
1·1
1·2
1·3
1·4
10⁴/T°K
ATOMS
MOLECULES

Fig. II. 5.

CHAPTER III.

Recombination of Oxygen atoms on Oxide Surfaces: Part 2. Catalytic Activities of the alkali metal Tungsten Bronzes, by P. G. Dickens and M. S. Whittingham.

Abstract.

The recombination of oxygen atoms has been studied on the surfaces of the alkali metal tungsten bronzes of general formula M_xWO_3 where M = Li, Na or K, and $0 < x \leq 0.80$. The recombination coefficients, γ, defined as the fraction of atomic collisions with the surface which results in recombination, were measured at 300°K by a side-arm method. Catalytic activities were found to be closely related to the electronic properties of the bronzes.

Recombination measurements were supplemented by studies of electrical resistance and crystal structure.

The activity of a catalyst may be determined by both electronic and geometric factors. The alkali metal tungsten bronzes of composition M_xWO_3, where $0 \leq x \leq 0.80$ provide an interesting series of graduated, stable, compounds in which the electronic properties change in a marked and controllable way but in which lattice parameters are only slightly affected. They are, therefore, useful systems to study in testing the role of the electronic factor in catalysis.

The crystal structure changes little with composition. The high x-value sodium and lithium bronzes have the perovskite structure (fig. III.1) and as x decreases the structure becomes progressively more distorted, passing through two tetragonal phases to the triclinically distorted structure of WO_3.[2] The Potassium bronzes have only tetragonal and hexagonal structures over their narrow composition range.[3] The electrical properties of the tungsten bronzes are well known.[4] They are n-type semiconductors for $x < 0.25$ and metallic conductors for $x > 0.25$ with one 'free electron' per alkali metal atom. This change in conductivity type may be correlated with the crystal structure. For $x < 0.25$ the alkali metal atoms may reside at the diagonally opposite corners of the cube; however when $x > 0.25$ the metal atoms must reside at corners on the same face of the cube. Here the interatomic distance is very similar to that in the pure metal e.g. for sodium 3.82 Å in the bronze against 3.72 Å in the pure metal. It is reasonable to suppose that the activity of the bronzes for oxygen atom recombination, which involves electron transfer between adsorbate and adsorbent will be composition dependent.

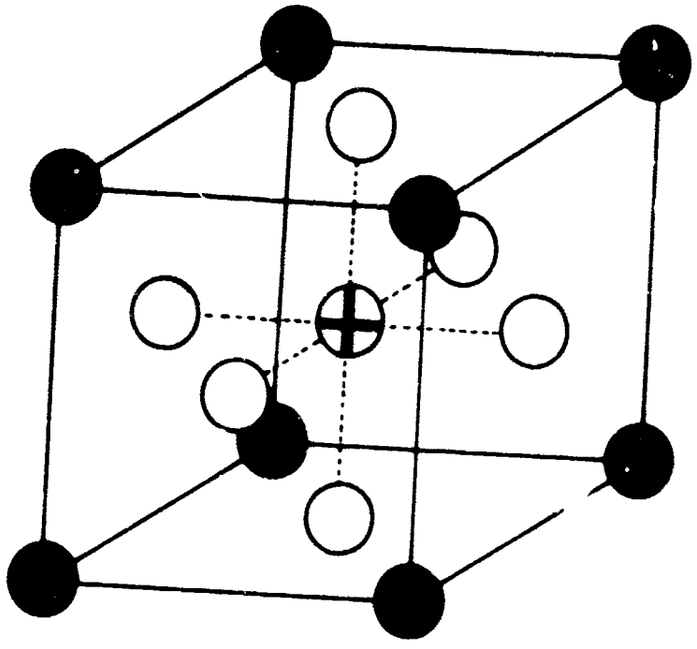

Fig. 1. Perovskite structure of $BaTiO_3$

●, Ba; ⊕, Ti; O, O.

The recombination of oxygen atoms on other oxide surfaces at room temperature has been found to be first order with respect to gaseous atoms.[1] The rate determining step is probably[1]

$$O(g) + O^{-}(ads.) \longrightarrow O_{2(g)} + e_{(solid)}$$

Experimental.

Atomic recombination coefficients were measured by the side-arm method of Smith[5] using an apparatus similar to that described in Part 1.[1] The side arm was enclosed in a water-jacket kept at 300° K, and the oxygen pressure was 28 μ. Samples of the catalyst were coated onto the inside of Pyrex cylinders from an acetone or water slurry of the powder. The Pyrex cylinders, which were 15 cm long x 3 cm diameter, fitted closely inside the side-arm. The method of measurement and calculation of the recombination coefficiences, is discussed in part 1.[1]

The bronzes were prepared according to the equation

$$\frac{x}{2} M_2WO_4 + \frac{3-2x}{3} WO_3 + \frac{x}{6} W \longrightarrow M_xWO_3$$

by heating the appropriate tungstate, tungstic oxide and tungsten powder in an alumina boat at 850°C under vacuum (10^{-5} torr) for five hours. A sample of pure tungstic oxide was heated in the same manner. The bronzes were washed successively with very dilute boiling NaOH, water, conc. HCl, water and acetone. Arc spectra showed the presence of less than 0.2% of impurities (alkali metals and molybdenum) in the starting materials. The sodium tungsten bronzes were analysed for sodium content using neutron activation analysis with sodium carbonate as standard. The 2.76 MeV peak was counted using a γ-spectrometer scintillation counter. The lithium and potassium bronzes were analysed

for alkali metal content by flame spectrophotometry using a Unicam SP 900 model. These bronzes were brought into solution by fusion in 1 Na_2CO_3:3 $NaNO_3$ mixture. Standard solutions were made from lithium or potassium nitrate and sodium nitrate to match the sodium content of the unknown solutions from the fusion mixture.

Surface areas of the powders were determined by the B.E.T. method using krypton adsorption at liquid nitrogen temperatures. The value 19.5 $Å^2$ was used for the area of a krypton molecule.

X-ray photographs were taken with a Guinnier-de Wolff camera using CuK_α radiation with exposure times of 72 hours; thoria was mixed with the samples to act as a standard.

The electrical conductivities of pelleted samples were measured at 10^{-5} torr using a Wayne-Kerr R.F. Bridge and an Avo electrical test meter. Measurements on the R.F. Bridge were restricted to resistances over 25 ohms. Measurements on pellets are unsatisfactory for low resistance materials, when the intergranular resistances may be relatively large. The resistances of the samples fell sharply from pure tungstic oxide to the metallic bronzes, table 1. This is in agreement with previous results.[4]

Results.

Within experimental accuracy, oxygen atom recombination was found to be first order with respect to gaseous atoms at 300°K on all the surfaces studied. Table 1 lists the values of the recombination coefficients, which are the mean of four runs on two samples and their standard deviations; the surface areas which are the mean of two

Table 1 Collected Results

COMPOSITION		SURFACE AREA	RECOMBINATION COEFFICIENT	SPECIFIC RESISTIVITY	CRYSTAL STRUCTURE*
Nominal	Analysed	m^2/gm	$\gamma \times 100$	OHM-CM	
WO_3	-	2.247	3.71±0.01	5200	WO_3
Na 0.10	0.102	0.317	2.61±0.08	150	I
Na 0.20	0.212	1.304	1.89±0.02	25	I,II
Na 0.25	0.260	-	1.83±0.08	-	-
Na 0.30	0.313	1.476	2.58±0.11	<10	II
Na 0.40	0.402	-	3.94±0.50	-	II
Na 0.45	0.454	1.582	4.26±0.36	<10	-
Na 0.50	0.500	-	3.82±0.03	-	(II),C
Na 0.60	0.600	0.767	0.70±0.03	<10	C
Na 0.80	0.801	0.400	0.42±0.02	<10	C
Li 0.05	0.026	2.247	5.60±0.44	-	WO_3
Li 0.10	0.086	0.125	2.86±0.33	-	I
Li 0.15	0.130	0.112	2.76±0.01	-	I
Li 0.25	0.217	0.228	2.15±0.02	-	I, (C)
Li 0.30	0.262	0.239	2.87±0.01	-	(I), C
Li 0.35	0.295	0.208	2.96±0.04	-	(I), C
Li 0.40	0.348	0.213	3.91±0.19	-	-
K 0.40	0.399	0.065	3.93±0.05	-	-
K 0.475	0.474	0.267	4.21±0.07	-	X
K 0.55	0.547	0.888	2.12±0.02	-	-

* I and II - tetragonal I and II phases [2], C - cubic, X - some less symmetrical system.

determinations; the electrical resistivity at room temperature; the analytical data and the x-ray structures.

Discussion.

Oxygen atom recombination is a very rapid reaction and so only the exposed outer layers of the catalyst surface are likely to be available for reaction. Some evidence for this is provided by the potassium bronzes which have similar activities to the sodium compounds and yet have very different surface areas. A quantitative expression for the effect of surface area on recombination coefficient is derived in the appendix. Fig. III.3, compiled from this expression, shows that the overall activity pattern is insensitive to changes in surface area.

Fig. III.2 shows that the pattern of catalytic activity for oxygen atom recombination is approximately the same whether Mis, Na, Li or K in M_xWO_3. This is a clear indication that electronic factors dominate the catalytic behaviour. As the crystal structure is dependent on the alkali metal present, it cannot have any marked effect on the activity pattern. It is interesting to note that the changes in surface area correspond almost exactly to the changes in crystal structure.

The conduction band in the bronzes can be considered as made up either by overlap of the alkali metal p orbitals[6] or by overlap of the tungsten 5d (t_{2g}) orbitals.[7] The former suggestion seems the more likely as the lattice dimensions permit appreciable overlap of the alkali metal p-orbitals, whereas little overlap of the tungsten 5d orbitals would be expected.[6] However only when there are sufficient alkali metal atoms, $x > 0.25$, will appreciable overlap of p orbitals be possible.

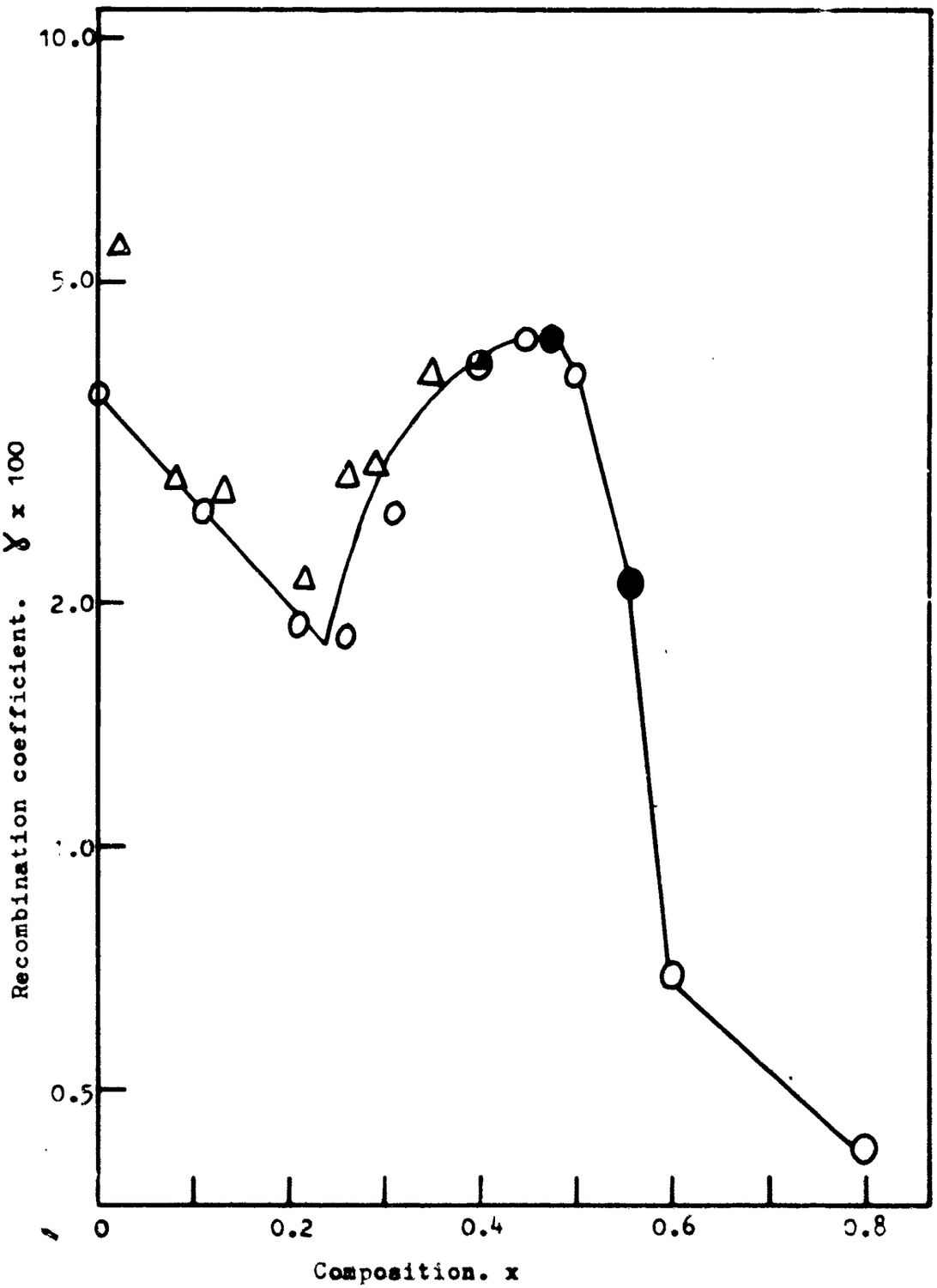

Fig.2. The recombination coefficients of the tungsten bronzes. Δ, lithium; O, sodium; ●, potassium.

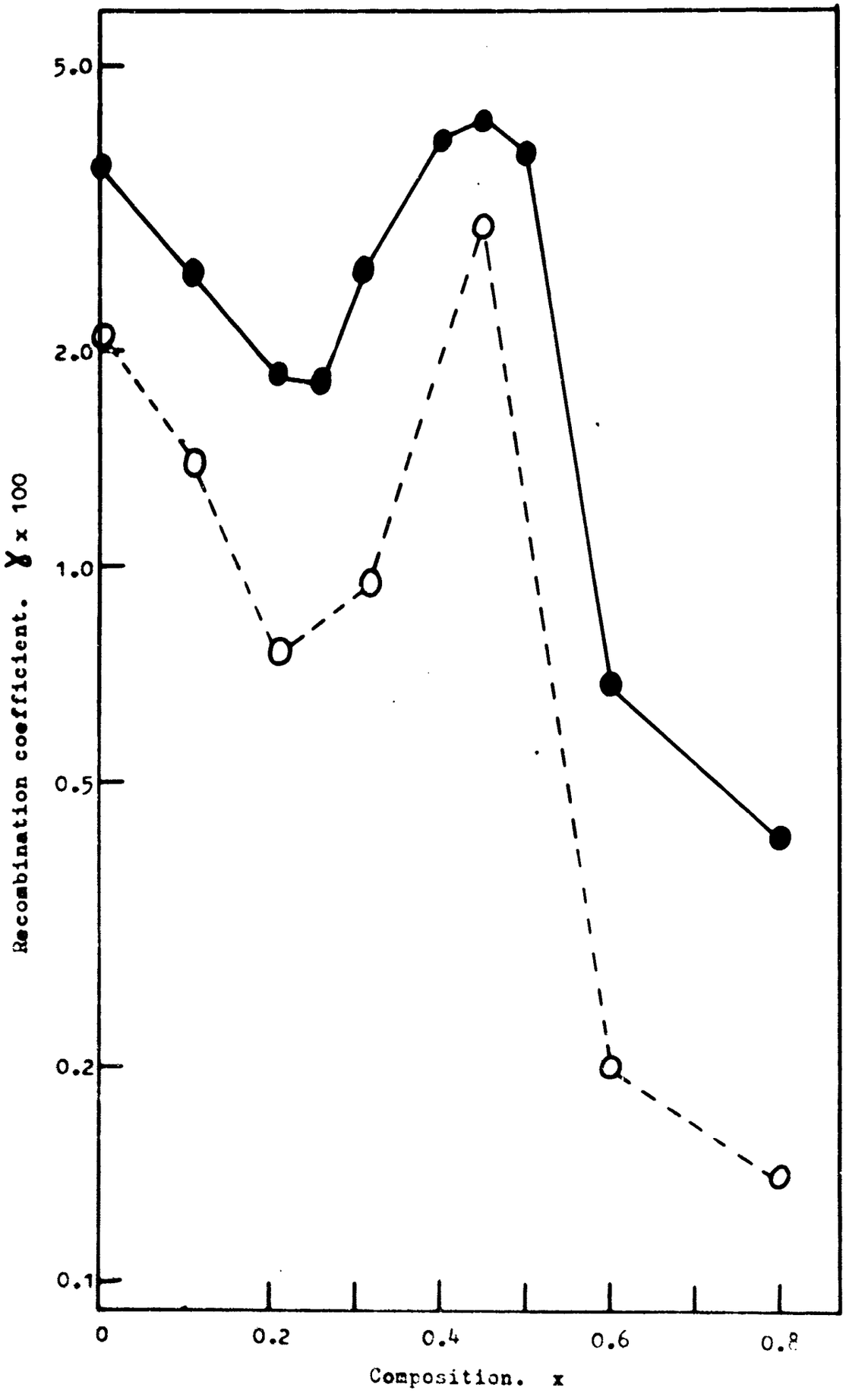

Fig.3. γ_o and γ_t for the sodium tungsten bronzes.

γ_o ——●—— ; γ_t - - -○- - -

When this occurs their energy will fall relative to those in the free atom. The s orbitals overlap appreciably with the filled WO_3 orbitals thus increasing their energy, by electrostatic repulsion, relative to the free atom. N.M.R. studies[11] show that the s orbitals of sodium do not contribute to the conduction band. For $x < 0.25$, the alkali metal electrons are localised and conduction will take place by a 'hopping' process probably involving some excited state in the WO_3 complex. Beyond this composition range the alkali metal electrons will become delocalised and metallic conduction will take place via the p-band.

It is probable that oxygen in the presence of oxygen atoms is adsorbed predominantly as $O^-_{(ads)}$ ions.[1] If the direct recombination reaction

$$O_{(g)} + O^-_{(ads)} \longrightarrow O_{2(g)} + e_{(solid)}$$

is rate determining, then low activation energy for this reaction and high coverage will promote the recombination rate.

In the semiconducting region, $x < 0.25$, the Fermi level will increase with increasing alkali metal content. According to the boundary layer theory of chemisorption,[8] oxygen will be adsorbed depletively to low coverages on n-type oxides, such as the bronzes within this composition range. The activation energy for the reaction is determined by the position of the Fermi level. As the rate depends exponentially on the activation energy, and directly on the coverage, which is proportional to the square root of the impurity content,[8] it is most probable that the effect of increasing activation energy will be dominant. Thus catalytic activity is predicted to decrease

from pure WO_3 to $Na_{0.25}WO_3$.

As x increases from 0.25 the alkali metal p-orbitals will become stabilised due to mutual overlap, and the Fermi level will decrease sharply. This will cause a decrease in the activation energy and an increase in the coverage. Hence the catalytic activity should increase sharply.

The p-band is thought to be fairly wide, ca 3eV[6], and so the energy levels within this band will be widely spaced. As the sodium content increases this band will fill and at some composition the Fermi level will reverse its general downward trend and increases in value again. This will cause an increase in the activation energy of the reaction and hence lead again to a decrease in the catalytic activity with increasing sodium content.

The measured values of the recombination coefficients thus confirm the general pattern predicted by the band theory.

APPENDIX.

The Effect of Surface Area on the Recombination Coefficients.

A simple model is postulated, comprising a cylindrical coating of powder with open-ended pores of length 2l and radius r. (Fig. III.4)

A is the total surface area/gm.

A_1 is the geometrical surface area/gm.

ρ is the measured density of the coating.

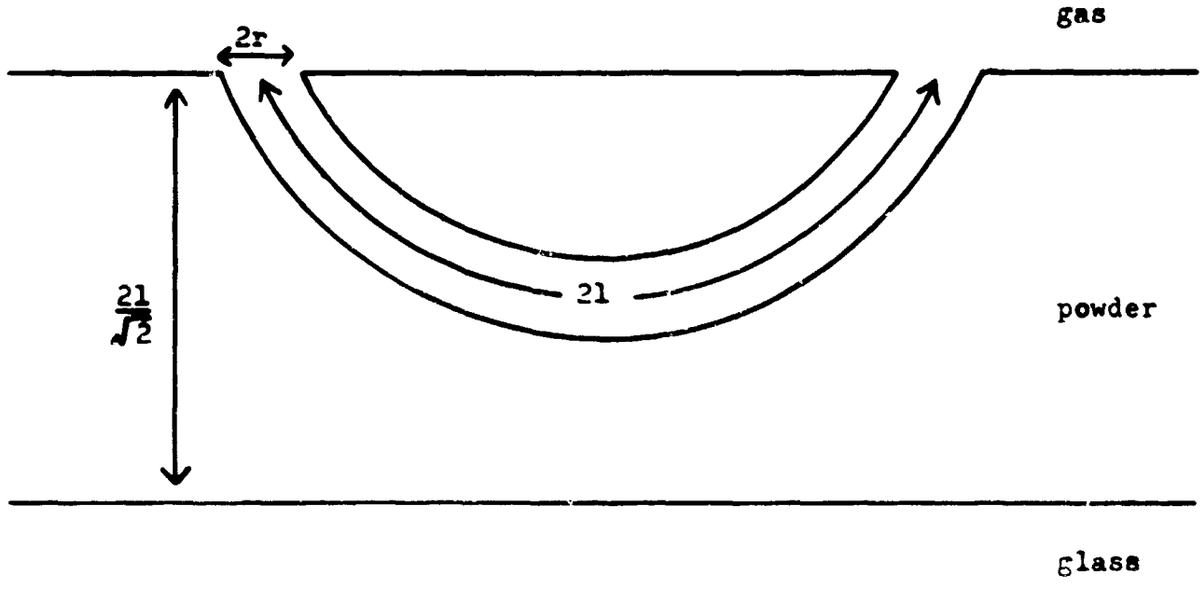

Fig.4. Dimensions of pore in oxide coating.

γ_o is the apparent value of γ calculated on the assumption that the area exposed by 1 gm. of material is the corresponding geometric area of cylinder, A_1.

γ_t is the true recombination coefficient, calculated on a basis of the actual available area/gm., A_2.

f is the fraction of surface used, A_2/A.

$\bar{v}$ is the mean speed of oxygen atoms in the gas phase.

n is the concentration of atoms in the gas phase.

Rate of reaction per unit area of cylinder $= \gamma_o \bar{v}n/f$

$= \gamma_t \bar{v}nA_2/4A_1$

$= \gamma_t \bar{v}nAf/4A_1$

Thus $\gamma_o = \gamma_t f A/A_1$

If diffusion is the only means of transport of reacting species into the pore then the change in concentration in the pore is

$$dn = -\pi r^2 D dx \, d^2n/dx^2$$

where x is the distance along the pore, and D is Knudsen's diffusion coefficient. At equilibrium, this is balanced by atom removal

$$\gamma_t \bar{v}n 2\pi r/2 = \pi r^2 D \, d^2n/dx^2$$

Using the boundary conditions $n = n_o$ when $x = o$ and that $dn/dx = 0$ at $x = l$ integration gives

$$n = n_o \cosh [h(1-x/l)] / \cosh h$$

where

$$h = l (\gamma_t \bar{v}/2rD)^{\frac{1}{2}}$$

Differentiating $dn/dx = hn_o/l \cdot \sinh[h(1-x/l)]/\cosh h$.

The rate of reaction per half-pore is the rate at which reactant flows in

i.e. $\pi r^2 D$ times the concentration gradient at $x = 0$

$$\text{rate} = \pi r^2 D \, n_o \tanh h/l$$

If the pore area were completely available the rate would be

$$2\pi r l \gamma_t \bar{v} n_o/4$$

Hence

$$f = 4\pi r^2 D \, n_o \tanh h/2\pi r l^2 \gamma_t \bar{v} n_o$$

$$= \tanh h/h$$

Now[8]

$$D = 2 r \bar{v}/3$$

and[10]

$$r = 2\theta (1-\theta) g/\pi A$$

where θ is the porosity of the material, g is the roughness factor, and assuming that the pore walls have the same properties as other surfaces. Hence the equation for recombination in the pores is

$$\gamma_o = \gamma_t A \tanh h/A_1 h$$

For the smooth surface $\gamma_o = g \gamma_t$. As θ represents the fraction of the geometrical area exposed to the atom flux by the pore mouths, the combined value becomes

$$\gamma_o = (1 - \theta) g \gamma_t + \theta \gamma_t A \tanh h/A_1 h.$$

The x-ray densities of the bronzes are about 7.2 gm cm^{-3}. The porosity of the coatings was slightly less than $\frac{1}{2}$, but the value $\frac{1}{2}$ will be used here for simplicity. The roughness factor will be assumed to have a value of 2. The pores are assumed to penetrate on an average half the distance from the coating surface to the glass cylinder. For a coating weight of 1.5 gm in a cylinder 15 cm long and 2.8 cm diameter.

$$l = 2.23 \times 10^{-3} \text{ cm}$$

$$A_1 = 62.3 \text{ cm}^2/\text{gm}$$

and

$$h = 70A\ \gamma_t^{\frac{1}{2}} \text{ where A is in } m^2/\text{gm}.$$

Hence

$$\gamma_o = \gamma_t \left[1 + 0.116 \tanh (70A\gamma_t^{\frac{1}{2}}) / \gamma_t^{\frac{1}{2}}\right]$$

In fig. 3 γ_o and γ_t are plotted against composition for some of the sodium bronzes. This shows that the variation in surface area from powder to powder does not alter significantly the pattern of the catalytic activities.

REFERENCES.

1. Dickens and Sutcliffe, Trans. Faraday Soc., 1964, 60, 1272.
2. Ribnick, Post and Banks, Non-Stoichiometric Compounds, Amer. Chem. Soc.. Advances in Chemistry, Series 39, 246.
3. Magneli and Bromberg, Acta Chem. Scand., 1951, 5, 372.
4. Shanks, Sides and Danielson, ref. 2, 237.
5. Smith, J. Chem. Physics, 1943, 11, 110.
6. Mackintosh, J. Chem. Physics, 1963, 38, 1991.
7. Sienko, ref. 2, 224.
8. Weisz, J. Chem. Physics, 1952, 20, 1483; 1953, 21, 1531.
9. Knudsen, Ann. Physik., 1909, 28, 999.
10. Wheeler, Adv. in Catalysis, 1951, 3, 250.
11. Jones, Grarbaty and Barnes, J. Chem. Physics, 1962, 36, 494, Narath and Wallace, Physics. Rev., 1962, 127, 724.

CHAPTER IV.

A Gauge to Measure Chlorine Pressures in the range 0.1 - 10 mm Hg.

By M. H. Booth and J. W. Linnett.

In the course of work on the recombination of chlorine atoms, it was found necessary to devise a gauge capable of measuring pressures of chlorine in the range 0.1 - 10 mm. Hg. This posed certain problems, since chlorine is a very reactive gas, attacking mercury and most other metals. The method of measurement had to be sensitive, and also give values of pressure independent of the nature of the gas. The latter condition was essential, since the gauge had to be calibrated against a Macleod gauge with a gas inert to mercury, and also since the pressures of mixtures containing chlorine and other gases would be required.

A capacitance method was chosen, since a proximity meter is obtainable which can detect very small changes in capacitance. The principle of the method is that small changes in level of a mercury U-tube manometer are recorded as capacitance changes. Each limb is about 4.5 cm. diameter. The mercury surface in the arm exposed to the chlorine is protected with a layer of dioctyl phthalate. The other arm contains a brass plate sealed into the glass so that its surface is a few millimetres above that of the mercury. These two surfaces form the condenser, the mercury being earthed via a tungsten seal, and dibutyl phthalate acting as the di-electric medium, since it has a fairly high di-electric constant (6.43 at 30°C) and a low vapour pressure. The brass plate is connected to the proximity meter. The total capacitance is of the order of 40pF, and the proximity meter can detect changes of 0.001 pF at maximum sensitivity. However, the most

sensitive ranges were not needed, and in any case require a very great control of mechanical stability and temperature. Even so, the gauge is on a rigid shelf of the wall, and is connected to the rest of the apparatus, which is subject to vibration from the rotary pump, by flexible tubing. Also, the gauge and the capacitance bridge box are enclosed in a thermostated perspex box.

The exact distance between the brass plate and the mercury surface can be altered by means of a mercury reservoir to give approximately the required range for a suitable sensitivity setting of the meter. To use the gauge, the reference arm is evacuated and isolated, a charcoal trap in liquid nitrogen ensuring a constant pressure. A suitable pressure range for a particular experiment is obtained by subjecting the gauge to the lowest required pressure, and balancing this out. The sensitivity is adjusted so that the highest required pressure is at the upper end of the scale. The gauge is then calibrated against a Macleod gauge, the calibration being linear except at the top end of the scale or at very high sensitivity values.

The gauge has been found to be quite satisfactory in use, giving reproducible pressure readings to 0.01 mm. Hg.